Stony Brook University

Duration of Reambulation Phases as a Modulator of the Detrimental Impact of Multiple Disuse Exposures on the Skeleton

A Thesis presented by

Surabhi Vijayaraghavan

To

The Graduate School

In partial fulfillment of the requirements for the degree of

Master of Science

in

Biomedical Engineering

Stony Brook University

August 2011

Stony Brook University

The Graduate School

Surabhi Vijayaraghavan

We the thesis committee for the above candidate for the Master of Science degree, hereby recommend acceptance of this thesis

Dr. Stefan Judex, Thesis Advisor

Professor, Biomedical Engineering Department

Dr. Yi-Xian Qin, Chairperson of Defense

Professor, Biomedical Engineering Department

Dr. Balaji Sitharaman, Committee Member

Assistant Professor, Biomedical Engineering Department

This thesis is accepted by the graduate school

Lawrence Martin

Dean of Graduate School

Abstract of Thesis

Duration of Reambulation Phases as a Modulator of the Detrimental Impact of Multiple Disuse Exposures on the Skelton

By

Surabhi Vijayaraghavan

Master of Science

in

Biomedical Engineering

Stony Brook University

2011

The detrimental effects of unloading on bone have been well-documented. Bone loss experienced by astronauts and bedrest patients can be as high as 3% per month. To design effective countermeasures without significant side-effects, the mechanisms by which unloading reduces tissue quantity and quality need to be understood. To this end, this study investigated whether the length of the reambulation period between successive exposures to unloading can mitigate, at least in part, the detrimental impact on the musculoskeletal system.

A genetically diverse adult female mouse population (F2 of BALB/cByJ x C3H/HeJ) was chosen to generalize findings across individuals with distinct genetic make-up. At 16wks of age, 30 animals were randomly divided into 2 experimental groups of n=15 each. Fifteen additional animals served as age-matched ambulatory controls (cf). Both experimental groups were subjected to 3 exposures to hindlimb unloading (HLU) of 3wks each. The first experimental group (3wf) was given 3wks of normal reambulation (RA) period between unloading cycles, while the second group (9wf) was subjected to 3 times as much reambulation time, 9wks, between successive exposures to unloading.

All mice were subjected to activity monitoring, *in vivo* computed tomography at the proximal and diaphyseal femur and abdomen, and *in silico* mechanical stress analysis, prior to and after each HLU. Control mice were subjected to the same procedures during the experimental protocol. Activity level, tissue morphology, and mechanical stress levels recorded indicated consistent deterioration during disuse. Generally, cortical sensitivity to disuse was an order of magnitude higher than that of trabecular bone to compression. Von-Mises mechanical stress experienced in the femoral distal metaphysis largely

echoed the trends exhibited by morphology, except that the cortex was more mechanically sensitive to unloading than trabeculae. Activity patterns indicated a remarkable similarity in spite of large differences in genetic makeup between individuals. Activity patterns were insensitive to the specific pattern of HLU/RU and showed only low to moderate correlations with changes in tissue morphology/stress. The magnitude of recovery tended to be proportional to the length of the RA period, with the 9wk recovery time being able normalize the tissue morphology to that of age-matched controls. Abdominal fat volume was greatly reduced by unloading while reambulation caused tissue recovery normal control levels even in mice subjected to only 3wk of RA.

In summary, a recovery period thrice as long as the duration of exposure can revert most harmful effects of disuse to the skeleton. Unfortunately, the longer reambulation period also restores bone's susceptibility to unloading while a much shorter reambulation period may suppress it. If confirmed by human studies, this data indicates a limited potential of optimizing reambulation periods between successive space missions.

TABLE OF CONTENTS

LIST OF SYMBOLS

AMB – Ambulatory (activity count)

AMD – Apparent (tissue) Mineral Density (mg/ HA cm^3)

aVMD - apparent Volumetric Mineral Density (mg/ HA cm^3)

BMD – Bone Mineral Density

BoneV – Bone Volume (mm^3)

BV – Bone Volume (mm^3)

BV/TV – Bone Volume fraction

CT – Computed Tomography

Ct. Ar – Cortical Area (mm^2)

Ct. Th – Cortical Thickness (mm)

DXA – Dual-energy X-ray Absorptiometry

Endo. Env – Endosteal Envelop (mm)

Endo. S – Endosteal Surface (mm^2)

Endo. V – Endosteal Volume (mm^3)

FEM – Finite Element Modeling

HLU – Hind Limb Unloading

Imax – maximum Moment of Inertia (mm^4)

Imin – minimum Moment of Inertia (mm^4)

LTM – Lean Tissue Mass (mm^3)

mo – months

Peri. Env – Periosteal Envelop (mm)

Peri. S – Periosteal Surface (mm^2)

Peri. V – Periosteal Volume (mm^3)

pMOI – principal Moment of Inertia (mm^4)

PVM – Peak Von Mises stress (MPa)

RA – Reambulation

ROI – Region of Interest

SAT – Subcutaneous Adipose Tissue volume (mm^3)

TAT – Total Adipose Tissue volume (mm^3)

Tb. N – Trabecular Number

Tb. Sp – Trabecular Spacing

Tb. Th – Trabecular Thickness (mm)

TMD – Tissue Mineral Density (mg/ HA cm^3)

TOT – Total (activity count)

VAT – Visceral Adipose Tissue volume (mm^3)

VOI – Volume of Interest

WBV – Whole Body Vibration

wk – weeks

LIST OF FIGURES

mean values, relative percentage changes over subsequent timepoints, and total percentage change in value from baseline (16wks). All values are expressed as Mean+SD.

Figure 12(a)(i): Page 41: Typifying morphological indices of the femoral mid-diaphysis: Ct. Th [mm] and Ct. Ar [mm^2] (Cortical Thickness and Area respectively) compared across the control (cf) and experimental (3wf, 9wf) groups in terms of mean values, relative percentage changes over subsequent timepoints, and total percentage change in value from baseline (16wks). All values are expressed as Mean+SD.

Figure 12(a)(ii): Page 41: Density parameter of the femoral mid-diaphysis: Ct. TMD [mg/HA-cm^3] (Cortical Tissue Mineral Density) compared across the control (cf) and experimental (3wf, 9wf) groups in terms of mean values, relative percentage changes over subsequent timepoints, and total percentage change in value from baseline (16wks). All values are expressed as Mean+SD.

Figure 12(b): Page 42: Morphological measures of the surface of the femoral mid-diaphysis: Endo. Ar and Peri. Ar, [mm^2] (Endosteal and Periosteal areas respectively) compared across the control (cf) and experimental (3wf, 9wf) groups in terms of mean values, relative percentage changes over subsequent timepoints, and total percentage change in value from baseline (16wks). All values are expressed as Mean+SD.

Figure 12(c): Page 42: Inertial quantification of the femoral mid-diaphysis: Ip[mm^4] (Principal Moment of Inertia) compared across the control (cf) and experimental (3wf, 9wf) groups in terms of mean values, relative percentage changes over subsequent timepoints, and total percentage change in value from baseline (16wks). All values are expressed as Mean+SD.

Figure 13(a): Page 43: Radial plots of correlation of trabecular (Tb.) and cortical (Ct.) parameters of bone volume fraction (BV/TV), thickness (Th.), and Tissue Mineral Density (TMD) with corresponding average activity measurements for cf, 3wf, and 9wf. Correlation percentages are expressed as squares of Pearson correlation coefficients. Radial axis indicates percentages while clockwise along the web, are the timepoints in weeks.

Figure 13(b): Page 43: Radial plot of correlation of principal Moment of Inertia (Ip) with corresponding average activity measurements, for cf, 3wf, and 9wf. Correlation percentages are expressed as squares of Pearson correlation coefficients. Radial axis indicates percentages while clockwise along the web, are the timepoints in weeks.

Figure 14: Page 45: Mechanical stresses experienced the femoral distal metaphysis: median VM stress and PVM [MPa] (VM – Von-Mises stress) compared across the control (cf) and experimental (3wf, 9wf)

increasing PVM from 0 to 2MPa. 31wks for 3wf and 43wks for 9wf denote completion of experimental procedure. Scale is as provided in the extreme left.

LIST OF TABLES

ACKNOWLEDGEMENTS

I would like to thank Dr Stefan Judex for being a wonderful advisor, for letting me find out the answers in my research myself, but stepping in to give me advice at exactly the right times. Importantly, I must thank him for trusting me more than I trusted myself, and for having me find out that I could do things I never remotely thought I could.

My sincere thanks to Dr Shikha Gupta, without whom lab would never have been the same to me; for being an amazing mentor, and guiding me ever-so patiently through all my mistakes.

A large thank you to Ms Alyssa Tuthill, for being the greatest person to turn to for anything and everything in lab, and for also being there with me through all that I never asked but she readily helped with. I will be grateful to her for showing me what efficient and proactive work is, simply and strictly only by example.

In this context, I have to thank everybody from all the bone labs for their ready help, advice, and guidance, for helping with my animals whenever I needed, and for making the lab such a lovely place to work in.

I have to mention my family for trusting me across 8000 miles, for letting my follow my heart and being supportive through my research and thesis process. My friends have been with me through thick and thin, and you guys are just too many to name here. You have been there for me at times when I needed you the most, even without your knowing I did.

Thank you!

1. INTRODUCTION

1.1 OVERVIEW – THE SKELETAL SYSTEM

The skeletal system, made up of highly specialized forms of connective tissue, acts as a support system for living organisms, specifically vertebrates. This system is primarily made up of cartilage and bone, sporadically different in structure (composition, mineralization states), but similar in function (bone formation, mineralization, and resorption). In addition to working towards the same central cellular activities, bone partakes in some peripheral functions like housing the hematopoietic system, and maintaining metabolic pathways associated with mineral homeostasis.

1.2 BONE

1.2.1 *Structure and Function*

Bone is composed of collagens, proteoglycans, noncollagenous proteins, and crystalline salts (, mainly calcium and phosphate). Bone is structurally stratified into cortical and cancellous/ trabecular compartments in terms of its components. Cortical or compact bone, composed of concentric lamellae of densely packed collagen fibrils, is responsible for mechanical and protective functions; while the trabeculae, a porous matrix of loosely organized spongy composition, is key to the metabolic functions. In this manner, the compartments are distinctly different in morphology and functionality. [1]

1.2.2 *Bone at the Cellular Level*

Bone basically consists of osteoblasts (from osteoprogenitor cells), osteocytes, bone lining cells, and those arising from the fusion of mononuclear precursors, the osteoclasts. The fully differentiated osteoblasts are responsible for mineralization and production of the bone matrix. Osteocytes, the most numerous in bone, are mature osteoblasts that partake in bone formation and maintenance to a limited extent, and can engage in inter-osteocyte communication. Bone lining cells are inactive, flat, elongated cells covering the surface of bone, whose functions are unclear yet. It is speculated that they might be precursors for osteoblasts. Osteoclasts which are large and multinucleated, lie on the bone surface, resorbing bone when active.

In summary, osteoblasts and osteoclasts trigger bone formation and resorption respectively, the two temporally and spatially related processes that adopt a pattern known as bone remodeling.

1.2.3 *Bone Remodeling*

Over the lifespan of a human being, bone formation is the primary dictating process over the first twenty years. For the following thirty years or so, the amount of localized bone formation and resorption are equal. Generally beyond this, the equilibrium called remodeling shifts towards resorption. The pace at which bone formation takes place slackens and begins to lag behind that of resorption. As this shift takes place, more bone is lost than formed. Consequently, skeletal mass reduces, trabecular connectivity reduces, hence reducing skeletal strength and making bone more susceptible to fractures and other long-term consequences.

1.3 MECHANICS OF BONE

1.3.1 *An Overview*

Bone architecture is influenced by its functions and stresses during normal weight-bearing. This architecture is considered optimal in design, its structure-function relationship is in perfect synchrony coupled with its role in mineral homeostasis under normal physiological conditions. Wolff's law brought in a more systematic definition, making light of the correlation between patterns in trabecular alignment and the direction of principal stresses estimated to occur during normal functions.[2]

Bone is viscoelastic, highly nonlinear, and anisotropic. This anisotropy triggers it to respond differently, making bone exhibit different properties, when experiencing loads from different directions.[3] This attribute makes bone dynamic, as it continually adapts to changes both in its physiological and mechanical environments. Hence, it is difficult to characterize its physical properties, or derive universal constants.

Bone properties can be classified into the material and structural. While the former is tissue-level and does not depend on the geometry or structure of whole bone, the latter depends on the entire bone, examining mechanical behavior and the way bone responds to forces applied in the natural environment. The former can be tested on uniform sections of bone, while the latter must be examined using whole bone.[4]

1.3.2 *Stress and Strain*

A force can induce acceleration or deceleration. While acceleration occurs when bone is unconstrained, deceleration occurs when the bone is constrained or there exists an equal and opposite force. Under deceleration, bone exhibits an internal resistance to the force, opposite in direction and equal in magnitude. This is distributed across the cross-sectional area of the surface on which load is applied, and is defined as *stress*.

$$\sigma = \frac{F}{A}$$

where σ represents stress, equaling the force (F) per unit area (A).

The SI unit for stress is Pascal (Pa), where 1 Pa = 1 N/m^2 = 1.45 X 10^{-4} psi.

Since force can be applied in any direction, it follows that stresses can develop in any direction. However, all stresses can be resolved into tension, compression, and/ or shear stress. Two forces directed against each other along one line produce *tension*, two forces in the same direction produce *compression*, and two forces against each other but along parallel lines produce *shear*.

1.3.2.1 ***Von-Mises Stress***

Von-Mises equivalent stress is the second invariant of the stress tensor generally used to predict plastic failure.[5] Because the resulting state of stress is rather complex and impractical to model and interpret using simple classical stress equations in our case, attention is focused on the peak von Mises (PVM) stress as a suitable representative. PVM is generally used to compare stress magnitude against material yield strength, and is calculated as:

$$\sigma_{eq} = \text{sqrt}\,[1/2\,((\sigma_{xx} - \sigma_{yy})^2 + (\sigma_{yy} - \sigma_{zz})^2 + (\sigma_{zz} - \sigma_{xx})^2 + 6(\sigma^2_{yz} + \sigma^2_{xz} + \sigma^2_{xy}))]$$

where

σ_{eq} – Von-Mises equivalent stress,

σ_{xx} – first component of stress (x-plane),

σ_{yy} – second component of stress (y-plane),

σ_{zz} -– third component of stress (z-plane),

σ_{yz} – fourth component of stress (yz-plane),

σ_{xz} – fifth component of stress (xz-plane), and

σ_{xy} – sixth component of stress (xy-plane).

1.3.3 ***Mechanical Properties of Bone***

As stated earlier, bone's dynamicity can be attributed to its anisotropy. It has been theorized that bone strength and rigidity are higher along the direction of customary loading. In context of bone, the femur

is oriented vertically. By functionality, it experiences vertical compressive loads, and in synchrony with its architectural design, cannot withstand transverse loads. This would most likely lead to high bending stress and consequently increasing fracture risk. Bone is less prone to plastic deformation when it experiences transverse loads, as it is more brittle.[6]

1.3.3.1 *Compartmentalizing Bone's Mechanics*

This is applicable within bone compartments as well, especially for the cortex, wherein osteons are oriented longitudinally as directed by bone's loading history.[7] Its important characteristic is its coherent strength in compression rather than tension. After maturation, its tensile strength and modulus of elasticity drop by 2% every decade.[8] As regards the trabecular compartment, its compressive strength is greatest parallel to the orientation of trabeculae in the femoral neck.[9] In contrast, in the lumbar vertebrae, it is highest when perpendicular to the axis of the lumbar vertebrae.[10, 11]

When the moduli of elasticity are contrasted for the trabecular and cortical components, a higher porosity for the former lends it a higher value than the latter. It follows from this that the less stiff trabecular bone is relatively rubbery and can withstand higher strain magnitudes. Owing to these subtle, nevertheless important, differences between trabecular and cortical compartments, it is important to specify both the strain rate and loading direction to obtain a comprehensive description of bone biomechanics.[12] Since bone is viscoelastic, its properties change based on the rate of loading as the material internally flows when a load is applied.

The mechanisms by which mechanical forces alter bone mass await clarification, but it has been proposed that the apparent density of a bone region is determined by its customary loading history.[13] This concept has been expanded by a mathematical model that relates bone mass at equilibrium to its typical loading experience. This daily history is defined as the sum of a series of loading events, each characterized by a load magnitude and number of cycles. Studies suggest that the effect of load magnitude should outweigh that of cycle number.[14]

1.4 BONE DISUSE

1.4.1 *An Overview*

Various models of physical exercise (overloading) preserve or increase skeletal mass. In contrast, reduction in mechanical use—as in sedentary people or in diseases associated with paralysis and unloading, such as prolonged bed rest and spaceflight—is associated with bone loss and is likely to result

in age-related osteopenia. Because gravity seems to be a major constraint, spaceflight has been judged the ultimate model to determine the role of gravity on the human skeleton.

1.4.2 ***Mechanism – Cellular Response***

Mechanisms for the variations in bone loss are yet to be understood clearly. Most studies at the cell level report bone resorption and a decrease in bone formation, thereby resulting in loss of bone mass.[15-18] Osteoblast population appears to decline immediately adjacent to the growth cartilage-metaphvseal junction, but osteoclast numbers are unchanged.[19] Studies of biochemical markers of bone turnover have been reported for a small number of subjects. Bone formation markers have been reported to increase to a point and remain constant over spaceflight, and decrease after return to normal ambulation.[20-23] In contrast, bone resorption markers have been reported to be increased during flight and unchanged or increased after flight. Thus it is not clear whether the bone loss is associated with increased bone remodeling, reduced bone remodeling, or an uncoupling between bone formation and resorption. The reported differences need not be contradictory.

1.4.3 ***Mechanical Response to Unloading***

Bone structure is adapted to provide maximum strength with respect to the spectrum of mechanical loads sustained during normal human activities. Because these loads change in extended weightlessness, both the total mass and the spatial distribution of bone mineral may change as well, with different rates of cortical and trabecular bone loss and variation between anatomic sub-regions of the same bone. Because bone strength depends on loading directions, material properties, and bone geometry, a redistribution of bone mineral may have a potential impact on bone strength at the conclusion of the flight.[24]

Recent in vitro studies suggest that bone cells are directly sensitive to microgravity.[25-27] It has been shown using organ cultures of living bone rudiments from embryonic mice that 4 days of spaceflight inhibited matrix mineralization, while stimulating osteoclastic resorption of mineralized matrix.[27] Current hypothesis includes one that says microgravity may alter mechanotransduction in bone cells by interfering with the formation of the cytoskeleton.[28]

1.3.4 ***Mechanotransduction***

Mechanotransduction is this process by which cells detect and react to mechanical signals. However, the mechanism behind this is not yet known. An outline of the process is based on the relationship between cellular activities, bone development and remodeling.

Mechanical loading on bone is sensed by certain cells that translate it into signals. These signals are transduced through the skeleton via sensory pathways which generate certain chemical signals that effect bone remodeling. The primary candidates for the bone sensory cells are bone lining cells and osteocytes.[29, 30]

Considerable evidence justifies optimism for the concept that regular physical exercise benefits the skeleton. Bone adapts to the loads applied to it. Despite physical training, bone loss is an adaptive process that can become pathological after recovery on Earth.[31] This adaptation includes an increase in density when mechanical loading increases and a loss of bone density when customary loads are removed. This concept has been expanded to a general theory of bone remodeling in which mechanical loading is a primary regulator.[13, 32, 33]

1.4.5 *Microgravity*

Microgravity-induced bone loss is similar to disuse-osteoporosis on Earth, which constitutes a challenging public health problem. Reduced mechanical use, because of hypodynamia (decreased forces) and hypokinesia (fewer movements), is the main factor leading to bone loss in space.[31]

1.4.5.1 *Implications*

Spaceflight-induced bone loss is a limiting factor for long duration missions, such as, an expedition to Mars or extended occupation of a space station. Before effective countermeasures can be devised, a thorough knowledge of the extent, location, and rate of bone loss during weightlessness is needed from actual space flight data or ground-based disuse models. In addition, the rate and extent that these losses are reversed after return from space flight are of great importance.[34] Accelerated bone loss in crew members in space is a well recognized effect of weightlessness on the skeletal system and a critical risk factor for the early onset of osteoporosis after return to Earth.[35]

1.4.5.2 *State of Current Data*

However, limited data is available about its precise nature and time-course, despite the many cosmonauts who have occupied space stations.[31] Existence in microgravity leads to cardiovascular deconditioning in humans, as indicated by the postflight reduction of upright exercise capacity and orthostatic tolerance.[36-38] Astronauts undergoing long-term spaceflight also experience loss of musculoskeletal integrity in load-bearing tissues[39] and reduced neuromuscular coordination during locomotion after flight.[40, 41] Studies document a net loss of bone mineral in the gravitationally unloaded skeleton of crew who had flown on short and long-duration missions.[21, 42-46] Similar deconditioning occurs during bed rest.[47, 48]

1.4.6 *Bedrest*

Long duration bedrest studies without exercise or other countermeasures show a similar, possibly less, bone loss compared to spaceflight. The spine, femur neck, trochanter, and pelvis mean BMD losses were about 0.9%–1.3% per month, while the loss from the legs and whole body were 0.3%–0.4% per month.[49] The calcium balance was about -180 mg/day, resorption markers were elevated, formation markers tended upward, but were not significant. 1,25 Vitamin D (vitD) and calcium absorption were decreased, and serum ionized Ca was increased.[50] The formation marker, osteocalcin, is elevated during short term bedrest.[51] Histomorphometry of bone biopsies taken before and after long duration bedrest indicated increased osteoclastic activity and decreased mineralization parameters.[52]

If we assume that the bone loss in bed rest is representative of the loss in space flight when countermeasures are not employed, then perhaps the hip and spine would lose about 10% bone mineral per year. Losses of this magnitude may still be acceptable if recovery were rapid. However, this is not the case. In addition, without the benefit of knowing how an individual will respond, while some individuals would lose considerably less than this, others could experience as much as 20%/year.[49]

1.4.7 *Recovery*

Bone is lost as a consequence of long-term bed rest in adults.[53] Limited available data indicates postflight bone recovery occurred in some individuals, but may require several years for complete restoration. Follow-up data in five individuals suggest that over a time period of 2–3 years, postflight bone recovery occurs in most but not all crewmembers. Although the data was not sufficient for statistical analysis, resorption bone markers appear elevated and formation markers decreased during 4 months of spaceflight.[54] Though calcium kinetics and bone biomarkers have been used to characterize bone health during spaceflight, no reports have addressed the impact of spaceflight on long-term bone health after spaceflight, i.e., the recovery of skeletal integrity, its nature and its time course.[55] Recovery can be expected, but the rate and extent will be individual and bone site dependent.[34] Although the bone loss may not be sufficient to increase the risk of fracture immediately on return, it may result in increased fracture risk at more advanced ages because of onset of age-related osteoporosis.[24]

1.5 FACTORS INVOLVED

1.5.1. *For Research in Space*

Although the information we have is a good beginning, additional spaceflight research is needed to assess architectural and subregional bone changes, elucidate mechanisms, and develop efficient as well as effective countermeasures. Current data indicate that several years may be required for complete recovery, which could impact on how often crewmembers may be assigned to missions. Assuming countermeasures are incomplete or not desirable, an alternate approach may be to accelerate recovery postflight. Therefore, methods to promote recovery should be investigated, e.g., exercise or anabolic agents.

The short- and long-term fracture risk from the known bone loss during space station stays of 4–6 months needs evaluation. This information would be useful for understanding how much protection is necessary during flights of this duration.

No countermeasures have proven entirely effective. It appears that the amount of exercise actually performed in space is highly variable and that the current information is very subjective. Considering the importance that load-bearing is believed to play in the maintenance of bone, techniques should be developed to accurately quantitate actual work performed in space.

Early computed tomography (CT) studies of cosmonauts suggest that the local distribution of bone loss in a given bone may be very inhomogeneous. A 6% change in BMD in the lumbar spine may represent much larger local losses. Therefore, in addition to routine BMD measurements, subregional measurements of bone mineral and or bone architecture should be investigated.[54]

A summary of the complications associated with spaceflight measurements are:

1. Number of subjects
2. Long time-frame
3. Crew focus
4. Activity conflicts
5. In-flight countermeasures
6. In-flight medical care
7. International crew
8. Crew rotation
9. Sleep/wake cycles

1.5.2 ***For Research concerning Bedrest Subjects***

Issues that prevent bedrest studies from being meaningful are again the variability in:

1. The nature and number of subjects

2. Duration of bedrest
3. Cause for bedrest (often due to physical and physiological disorders, thus making it difficult to delineating the effect of unloading itself, as against pre-existing health conditions)
4. Medical interventions over the period

1.5.3 ***Eliminating Humans – The Rise of the Animal Model***

Molecular geneticists are looking for ways to model human disease and companies testing new drugs are creating an unprecedented demand for inbred rodents. The rise of the mouse as biomedicine's model mammal has been incredible.[56] The need for such an animal model for disuse is only too obvious, keeping in mind the confounding complex factors (mentioned earlier) that make observations from human studies highly case specific.

NASA has developed a rat model to simulate on earth aspects of weightlessness like alterations experienced in space, i.e., unloading and fluid shifts. Comparison of data collected from space flight and from the head-down rodent suspension model suggests that this reproduces many of the physiological alterations induced by space flight. Data from various versions of the model are virtually identical for the same parameters; thus, modifications of the model for acute, chronic, or metabolic studies does not alter the results as long as the critical components of the model are maintained, i.e., a cephalad shift of fluids and/or unloading of the rear limbs.[57] This model enables good observations that cannot be made otherwise. [58]

The enormous potential for meaningful animal investigation has not been fully exploited. Only small numbers of immature animals have been flown at one time, and no longitudinal studies have been performed. Most studies have been observational. Animal experiments have been of relatively short duration(4–18 days) compared with human flights aboard Skylab (up to 84 days) and Mir (1 yr).[59]

1.5.4 ***Physiological Factors***

While bone loss as a result of disuse is well established, research is influenced by certain principal factors involved in the nature of exposure to disuse, these being:

1. Genetic make-up of subject exposed
2. Localization of response
3. Ageing
4. Duration of exposure
5. Number of exposures (and thereby, the pattern of exposure)
6. Gender

A study of disuse is made increasingly meaningful by exploring these factors.

1.5.4.1 *Genetics*

Genetics plays a role as much as 70% in osteoporosis[60, 61] and BMD[62]. Several candidates known to be involved in bone metabolism include the vitamin D receptor[63-65], type I collagen a1 gene[66], estrogen receptor[67], and interleukin-6[62]. Further, susceptibility to osteoporosis is influenced by transforming growth factor-beta 1.[68]

Measurements of bone loss vary extensively between crewmembers; some individuals incur losses equivalent to one-half the bone mineral they would lose in a lifetime of normal aging, whereas others show minimal to no change.[69] Striking inter-individual variations in bone responses suggest a need for adequate crew pre-selection.[31] Baseline bone morphometry and cellular activity modulate the degree of loss in the appendicular skeleton during disuse.[70] Genetics is even responsible for the site specificity in bone response to osteoporosis.[71] The effects of sciatic neurectomy and genetic regulation of bone response to mechanical unloading have been well documented. [72, 73] These include systemic changes, cellular bone forming parameters, again specific to the site under observation. [74] Strong evidence supports the existence of a skeletal mechanosensitivity gene in mice. [75]

QTLs are in progress to find the influence of genetics. Quantitative trait locus (QTL) analysis is a statistical method that links two types of information—phenotypic data (trait measurements) and genotypic data (usually molecular markers)—in an attempt to explain the genetic basis of variation in complex traits.[76, 77]

How This Study deals with Genetics

More than 70% of the variability in human bone density has been attributed to genetic factors as a result of studies with twins, osteoporotic families, and individuals with rare heritable bone disorders. Comparison of bone parameters among 11 inbred strains of female mice longitudinally through their lifetime to determine the extent of heritable differences in peak bone density revealed significant differences at each of the three sites investigated. Developmental studies of femurs conducted at 2, 4, and 8 months of age with 4 female strains showed differences in total density among strains at 2 months and thereafter.[78] While the C3H/HeJ strain has consistently exhibited the lowest sensitivity to unloading in almost all bone parameters, the BALB/cByJ is at the other end of the spectrum.

Various studies have reinforced the strong influence of genetic influence on inducing variability in bone loss.[70, 71, 79, 80] Hence, for this study, we have used a genetically diverse second generation F2

mouse population in-bred twice across the BALB/cByJ (most sensitive in terms of bone mechanics) and C3H/HeJ (least sensitive) strains that nearly spans the diversity in response (BALB/cByJxC3H/HeJ).

1.5.4.2 *Localization of Response*

While previous studies have defined the magnitude of total or integral bone loss at several skeletal sites, there is little information regarding the spatial distribution of these changes within specific skeletal sites. Such spatial heterogeneity has been observed in the tibias and femorae of rats undergoing hindlimb unloading (HLU),[81] and differential cortical and trabecular tibial bone loss in cosmonauts[31].

A 5-year follow-up study of the Skylab astronauts indicated further loss of bone density from the heel in those who originally had only modest changes immediately post flight, with little recovery in those astronauts who had the greatest decrements post flight.[82] Thus, data suggests that the bones most stressed by gravity (e.g., calcaneus, tibia) are likely to be most affected by weightlessness, that the loss in bone mineral from such bones may be progressive, at least over 6 months, and that recovery is slow and may not be complete even after 5 years. As is discussed further, these conclusions are supported by human bedrest studies and nonprimate animal studies.

Limited BMD measurements documented that bone was not lost equally from all parts of the skeleton. Subsequent studies have documented the regional extent of bone loss. Bone loss was detected in the calcaneum, and not in the arm in three Skylab mission crew studied. [83] These studies demonstrated mean losses in the spine, femur neck, tibia, trochanter, calcaneus, and pelvis (of about 1%–1.6% and 0.3%–0.4% per month from the legs and whole body over long-duration Russian flights[54]) with large differences between individuals as well as between bone sites in a given individual. Segmental analysis of the total-body scans showed significant loss in the lumbar spine, total spine, pelvis, trunk, and legs. [69, 84] However, a fall in BMD values in the pelvis, femoral neck, and trochanter were reported, with no significant whole body bone loss in cosmonauts who spent 131–312 days on the MIR space station.[84] While three of nine Skylab crewmembers lost statistically significant bone mineral from the calcaneus, there was no loss seen in the radius or ulna. This may have occurred because of the low percentage of trabecular bone at the measured sites or because the distal arms are functionally non-weight-bearing bones and were continually and extensively used.[54]

Specific studies have been conducted with respect to spaceflight, where cortical and trabecular bone respond to mechanical unloading.[85] Compartment-specific response is another aspect of localization of bone response to disuse. However, early on, BMD measurements were primarily recorded by DXA, which represents the sum of trabecular and cortical compartment losses by area. It lacked information

on how the envelopes are affected by spaceflight, and hence could not probe compartment-specific loss.[24] 4-12 month studies using this modality produced average bone loss rates of 1%/month in the spine and 1.5%/month in the hip.[69, 86] Subsequently, cortical and trabecular bone loss was measured using QCT, enabling the characterization of subregional distribution of vertebral and proximal femoral bone loss. In 4- to 6-month flight, cortical bone mineral loss in the hip was found to occur primarily by endocortical thinning. In the hip, cortical and trabecular vBMD (v-volumetric) loss rates were 0.4–0.5%/month and 2.2–2.7%/month, respectively. In contrast, losses in the spine were less significant.[24]

To determine the rate and extent of bone loss and recovery from long-term disuse and in particular from disuse after exposure to weightlessness, bed rest is used to simulate the reduced stress and strain on the skeleton. Potential redistribution of bone mineral was observed: during bed rest, the bone mineral increased in the skull of all subjects. Although the majority of areas showed positive slopes during reambulation (RA), only the calcaneus was significant with nearly 100% recovery. The pelvis and trunk were also significant, but did not recover as much. The change in total BMD and calcium from calcium balance was significantly correlated.[49]

How this Study deals with Site-Specificity

The greatest bone losses have been observed in the lower appendicular skeleton, specifically in pelvic bones, lumbar vertebrae, and the femoral neck.[49, 87] Based on these site-specific changes, the regions most sensitive to unloading have proven to be the calcaneus, trochanter, femoral neck and tibia, in that order (with the trochanter and femoral neck being almost similar in their variations). Likewise, recovery is most significant in the lumbar spine, followed by the femoral neck. Hence the femur is a location of strategic interest that is pivotal to variations in exposure to unloading and RA. This study focuses on femur and abdominal fat as indicative and important sites of response to unloading, with due consideration given to the roles played by trabecular and cortical components.

1.5.4.3 *Ageing*

The growing animal skeletal unloading results in a temporary inhibition of bone formation. Within 2-5 days of unloading, osteoblast numbers, longitudinal bone growth, and the rate of calcium accumulation in bone are significantly reduced.[88, 89] However, after 12-14 days of unloading, bone formation, as judged by these same parameters, returns to normal.[90] Unlike the adult, the temporary inhibition of bone formation induced by skeletal unloading does not result in a loss of bone per se but rather a temporary slowing in the accumulation of bone that manifests itself as a deficit in total bone calcium compared with age-matched, normally loaded animals. The deficit in bone calcium induced by skeletal

unloading in the growing rat is sustained for at least 4 weeks (wk) and presumably as long as unloading is sustained.[88]

How this Study deals with Ageing

When the suspension model is used in the context of spaceflight, it is only meaningful to use adult mice in order to be able to extrapolate the inferences to the human astronaut case (average astronaut age as per NASA: 26-46yrs, average: 34yrs), to eliminate the afore-mentioned role of the growing skeleton in bone response to unloading. Consequently, all animals used in this study will be 4mo old at experimental baseline.

1.5.4.4 *Duration of Exposure*

During the 3 skylab flights in which BMD was obtained, the loss of bone density from the calcaneus was greater in the 84-day flight than in the shorter flights, ranging from +0.7% to -7.9%.[91] Similar losses were observed in the Salyut-6 cosmonauts, with total decrements from -0.95 to -19%; the losses were greater in the 140- to 184-day flights than in the 75-day flight.[92] Broadband ultrasound attenuation(BUA) of the calcaneus of the euromir cosmonauts reduced 7.34% and 13.18% respectively for the 1- and 6-month periods.[3] Their bone densities fell 2.27% and 4.5% respectively, in the trabecular bone of tibia, with a 1% gain (1-month) and 2.94% loss (6-month) in the tibial cortex.[22] However, changes in bone density in the radius and ulna of the Skylab astronauts, and in the radius of the euromir cosmonauts was minimal[22, 91]; similarly, changes in the lumbar spine of the cosmonauts following extended spaceflight was minimal[93]. Interestingly though, for cosmonauts in space for a time (311 and 438 days) significantly longer than the average time of 4–6 months, the rate of bone loss from the spine was about half the overall average, indicating a decreasing rate of loss, while the changes in the femur were similar to the overall average, indicating continued bone loss.[54]

How this Study deals with Duration of Exposure

This study analyzes the effect of varied durations of exposure to disuse by incorporating this as a variable parameter in its experimental design.

1.5.4.5 *Multiple Exposures*

Data from crewmembers –a small number of whom flew on more than one mission – was used to analyse changes in BMD between different sets of pre- and postflight measurements. Plotted as a function of time (days after landing) for the lumbar spine, trochanter, pelvis, femoral neck and calcaneus, averaged losses of bone mineral after long-duration spaceflight ranged between 2% and 9% across all sites with recovery models predicting a 50% restoration of bone loss for all sites to be within 9

months.[55] Actual BMD did not depend on preceding cumulative periods spent in space. During recovery, tibial bone loss persisted, suggesting that the time needed to recover is longer than the mission duration.[31]

Current research has focused solely on the effects of a single spaceflight (, just the period of disuse over spaceflight, or the period of spaceflight itself and the period of recovery on return to normal ambulation afterwards), in spite of astronauts commonly being assigned to multiple space missions spanning through their career.[94] But since the detrimental effects of spaceflight have been declared with certainty, prior exposures to disuse can only worsen the degree of bone health. The net consequences of these repeated exposures remain to be investigated.

How this Study deals with Multiple Exposures

This study is based on prior evidence that clearly outlined the benefits of staggered exposure to disuse over a single exposure when the total duration of exposure to disuse was the same. Transitively, it also professed an increasing degree of damage when the number of exposures to disuse increased. [95]

1.5.4.6 *Gender*

There is minimal evidence that spaceflight increases bone resorption at either cortical or cancellous bone sites in growing male rats.[96] In contrast to males, the osteoclast number increased in pregnant growing rats.[97] Spaceflight accelerated OVX-induced cancellous bone loss in the proximal tibial metaphysis and induced bone loss in the epiphysis.[98, 99] The bone loss in the metaphysis of OVX rats was due to excess bone resorption; there was no reduction in bone formation.[98] These results suggest that there may be sex differences related to gonadal hormone levels that influence the skeletal response to spaceflight. Much research has gone on to establish that the female mouse is more resilient.

How this Study deals with Gender

In correlation with sound existing research in this domain, it was decided to study female mice solely for their activity and morphology patterns.

1.6 EXISTING COUNTERMEASURES

In order to assess the effects of all of these factors on bone, investigators have been trying to unravel the mechanisms behind bone remodeling and architecture.[100] Obviously, there is a need for selective and predictable locally-active anabolic agents that can tip the scales of bone remodeling in the direction of an equilibrium again.[1] Treatment strategies hold implications for the ever-multiplying osteoporosis case apart from spaceflight.[31]

1.6.1 Exercise Regimen in Space

Despite the prescription of an intense exercise regimen designed to maintain mechanical loading of the skeleton, crewmembers on the Soviet/Russian MIR space station lost aBMD (a-areal) at an average monthly rate of 0.3% from the total skeleton, with 97% of that loss from the pelvis and legs.[101] It is not known what the bone loss would be without the exercise program, but it is not sufficient to prevent significant bone loss.[54] Strength testing before and after each flight documented the apparent effectiveness of the exercise program to protect the muscles. However, bone loss continued. The rate of loss from the calcaneus, however, was less than that found during ground-based bed rest studies, suggesting that these exercise countermeasures may have been at least partially successful. [40] On the other hand, overall the calcium loss was not ameliorated by these countermeasures.[43]

However, exercise protocols and equipment for astronauts remain subjects of research because no current regimen fully prevents deconditioning.[102] There may also be other situations when the crewmembers cannot exercise, e.g., injury, equipment failure or sickness.[103]

1.6.2 Pharmacological Interventions

Pharmacological interventions, thus far, revolve around drug families of bisphosphonates, pyrophosphate, estrogen analogs, fluorides, and potent parathyroid hormone (PTH). These generally operate by lengthening osteoblast working lives, inhibiting osteoclasts, or increasing BMD.[104] However, among the major concerns with their use is the potential for upper GI-related events, involving the stomach, duodenum, or esophagus, renal and liver dysfunctions, osteonecrosis, and osteomyelitis.[103-106] Additionally drug research is primarily directed towards osteoporosis and bone fracture, over alleviating the effects of microgravity.

Several animal models for microgravity have been tested with these drugs as a test for their anti-unloading effects[107] and bedrest models. A combination of alendronate with exercise might reduce the time needed to protect the skeleton, but needs investigation. Cellular activity measurements showed that in completely immobilized men, the mineralization rate was lower than in controls without change in osteoid parameters; in contrast, osteoclastic parameters were increased. In immobilized men given the training program, bone formation was normal and bone resorption was increased. In immobilized men treated with diphosphonate, osteoid parameters and resorption activity were decreased. In immobilized men with diphosphonate plus training, the osteoid parameters and the resorption activity were reduced but to a lesser degree than in immobilized men with diphosphonate alone. However, a decrease in mineralization rate and an increase in bone resorption activity were

found in both studies. Exercise stimulated bone resorption and diphosphonate inhibited the osteoclastic activity. These data emphasize the difficulties in finding good models to stimulate spaceflight conditions on earth. Comparative studies must be done using bone biopsies to determine more precisely the effects of weightlessness on the human skeleton.[52]

1.6.3 Whole Body Vibrations

Whole body vibrations (WBV) are, of late, being explored as viable counter mechanism against bone loss.[108-111] Chronic vibrations tend to increase stiffness, hardness, and modulus of elasticity. Small oscillatory accelerations enhance bone morphology as a consequence of increasing osteoblast activity.[109] Increasing magnitudes of WBV were associated with a non-dose-dependent increase in trabecular bone volume (BV/TV) at the proximal tibial metaphysis, although other sites (femoral condyles, distal femoral metaphysis, proximal femur, and L5 vertebral body) were unresponsive. If this non-dose-dependent phenomenon is verified by future studies, it suggests that a range of magnitudes should be examined for each application of WBV.[112] Nevertheless, excessive, chronic WBV has a number of negative side effects on the human body, including disorders of the skeletal, digestive, reproductive, visual, and vestibular systems. Whole-body vibration training (WBVT) is intentional exposure to WBV to increase leg muscle strength, BMD, health-related quality of life, and decrease back pain. ISO standards indicate that 10 $min \cdot d^{-1}$ WBVT is potentially harmful to the human body.[113]

1.7 ACTIVITY

Though activity monitoring in disuse studies is a fairly new concept, several studies have made fleeting mentions of activity in the context of increasing calcium accretion caused by bone formation occurring over reloading, considering the absence of evidence of a significant role played by bone resorption over the same phase. While reloading increases the rate of bone formation at the tibiofibular junction, the response is gradual, with the maximum increase in formation occurring after 12 days of reloading. The lag in bone formation may be, in part, a consequence of the animal's propensity to lie quietly in its cage and not move about during the 24-48 hrs immediately after reloading. This is the level at which current research stands with respect to a possibly much more significant role played by activity. [31] Little is known about the relationship between walking characteristics, skeletal loading, and bone maintenance in humans, even in other situations like stroke.[114]

Devices for monitoring activity have evolved greatly over the years.[115] The success of a project greatly depends on the forethought devoted to achieve the sampling algorithm for observing the study of

behavior.[116] An optimal compromise between the nature of variables explored and the innate properties of the model is essential to this end. [117]

Activity monitoring based on motion sensors, traditionally used in human and animal research, has been used in a wide range of fields ranging from magnetic resonance imaging to cardiology. For most part, these are accelerometer-based human studies. [118-120] The Columbus Instruments, IR-sensor based Opto-M3 system is a fairly new modality, primarily aiding adiposity and neurology research. [121-124]

1.8 MOTIVATION BEHIND THE STUDY

Compounding all the above-stated factors, there is a pressing need for a comprehensive analysis of the detrimental effects of multiple exposures to disuse to bone, and the variations in recovery patterns over different periods of intermittent phases of normal loading in the context of astronauts and space research, and bedrest patients.

This study attempts to target this issue by means of a well-documented and well-research animal suspension model, with a genetically diverse population that would mitigate subjectivity induced by unique responses exhibited by different genetic strains. This will study the effects of 2 different periods of normal loading between equal durations of unloading. Micro-architectural properties of the femur chosen to represent the lower appendicular skeleton, the region that bears the most significant damages caused by unloading. Two sites, the distal metaphysis and mid-diaphysis, will be observed to study localization in response to weight-bearing. These properties will be quantified and compared by computed tomography (for morphology) and finite element analysis (for mechanical response, that provides a more wholesome picture of bone response). These measurements and animal activity will be monitored longitudinally to account for age-dependent and seasonal variations. The trabecular and cortical compartments at both sites will be contrasted to understand the mechanism behind bone remodeling under unloading better.

With this in mind, the following are the specific aims of the project.

2. SPECIFIC AIMS

GLOBAL HYPOTHESIS

The period of intermittent exposure to normal ambulation between disuse, controls recovery of bone quality and quantity in a time-dependent manner.

2.1 HYPOTHESIS 1

Individual variability in animal activity becomes inconsequential when comparing populations subjected to different loading environments.

Specific Aim 1

To study activity patterns through subsequent suspension and recovery; and observe the extent of variability introduced by outliers within populations exposed to the same lifestyle. Transitively, to observe the effects of extraneous animal activity across populations experiencing different load-bearing environments. Also, to determine if the degree of decline in activity is progressive following consecutive suspensions irrespective of recovery period or if activity might be enhanced relative to previous suspension owing to acclimatisation to suspension. Also of interest is the probability of faster stabilization in adapting to normal activity immediately following release from suspension.

Two groups of adult female mice (4mo) (n=15) will be subjected to three equal durations of HLU (3wk) with group 1: 3wk, and group 2: 9wk of RA between each HLU, and compared with age-matched ambulatory controls. The groups will be monitored for activity at multiple time points prior to suspension and, after release, against age-matched controls in an Opto-M3 Triple Axis cage system. Activity values will be assessed for time-dependent trends in recovery patterns suggestive of a definitive improvement, maintenance or deterioration spanning through the duration of the experiment; variations within each post-suspension adaptation interval; and bias of the effects of unloading towards planar versus vertical motion, if any. The crucial underlying rationale for acitivity monitoring is that variations in structural and mechanical response due to individual genetic make-up might be accounted for by activity.

2.2 HYPOTHESIS 2

Prolonging recovery periods between multiple exposures to disuse enhances recovery of bone strength and reduces decline in musculoskeletal properties.

Specific Aim 2

To determine the importance of reambulation periods between consecutive periods of unloading on skeletal morphology, whether longer reambulation can improve bone recovery or if reambulation per se is essential for recovery regardless of duration.

This specific aim will be conducted in conjunction with SA1. In vivo microCT and finite element analysis will be performed across multiple skeletal sites prior to and after release from HLU. Analyses will focus on temporal associations between tissue recovery and site-specific morphology and strength.

2.3 HYPOTHESIS 3

The effects of disuse on musculoskeletal properties reflect uniformly on the animal's activity.

Specific Aim 3

To determine the relationship in terms of strength of correlation between activity values recorded in SA1 and the various morphological and mechanical indices analysed in SA2. Additionally, to infer from patterns in strength of correlation about the trends among experimental and control groups, across the trabeculae and cortex, over phases of disuse and normal loading. Also to detect the possibility of a decisive trend of association between activity values and a key physiological parameter.

3. MATERIALS AND METHODS

3.1 EXPERIMENTAL DESIGN

Adult (4mo old) second generation cross-bred F2 female mice (BALBxC3H) were bred in litters of 3-10 and randomized between the control (cf) and experimental groups (3wf and 9wf) with n=15 per group (, where "f" = female, "c" = control, "w" = number of wks of RA between consecutive exposures to HLU). (Fig. 1) The 3wf group was subjected to 3 exposures to HLU of 3wks each, the first two followed by 3wks of RA. The 9wf group was subjected to 3 exposures to HLU of 3wks each, the first two followed by 9wks of RA.

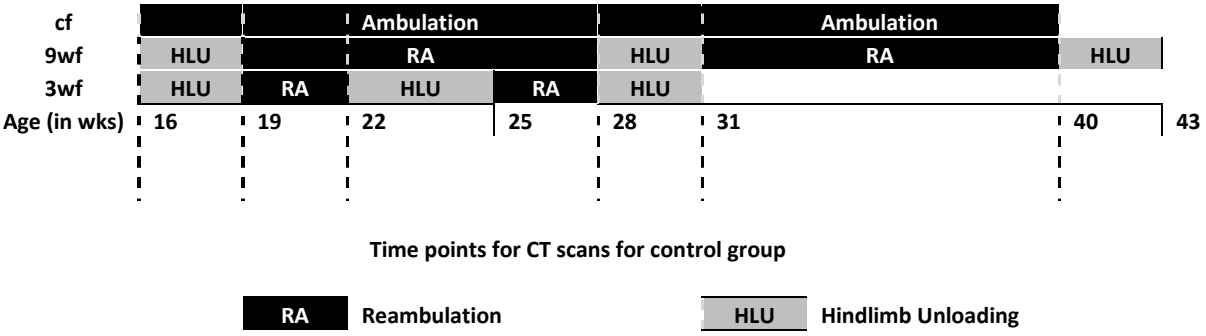

Figure 1. Block diagram depicting the experimental design for the 3 specific aims, where cf = control group, 3wf and 9wf = experimental groups.

The animals from the experimental groups underwent longitudinal *in vivo* Computed Tomography (CT) and activity monitoring scanning before and after every HLU period while the control groups were scanned and monitored for activity at an equal number of timepoints as each of the experimental groups (to ensure equal exposure to radiation through the experiment duration). These timepoints are marked with a dashed line in the diagram above.

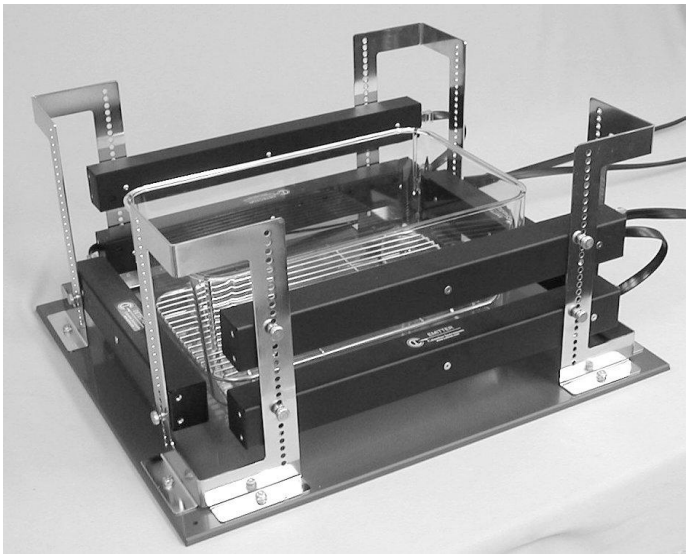

Figure 2. Activity monitoring system between each individual animal cage is positioned.

3.2 ANIMAL CARE FOR NON-SUSPENSION ANIMALS

With non-suspension animals referring to both the normally ambulating controls and experimental groups going in RA, all these animals were single-housed in standard mouse cages with easy access to rodent chow and water. Weights were recorded biweekly to monitor their health.

3.3 ACTIVITY MONITORING

Animal activity was monitored using the Columbus Instruments 16-chamber Triple Axis Opto-M3 system (Fig. 2), the operating principle being 1 serial whole-number counter increment for each interruption of the infrared (IR) beam across the cage, caused by animal movement. These motion sensors were placed along the 3 coordinate axes, returning 2 parameters: ambulatory (AMB) and total (TOT) counts. Each time a beam was broken, TOT incremented by 1 count. AMB count accumulated each time a new beam was broken. AMB did not respond to the same beam being broken and restored repeatedly, thereby preventing AMB from responding to rapid beam interruptions caused by scratching, grooming, digging, or other stereotypic non-ambulatory movements.

By recording the counts accumulated by the TOT and AMB counters, it was possible to compare amounts of ambulatory and stereotypic movements. Across the coordinate axes and 2 parameters, a 3-fold output was generated, namely XY AMB, XY TOT, and Z TOT. The animals from the 3wf and 9wf groups were placed in the activity monitoring system 1 day prior to HLU and on the 4th day of RA post release from suspension. cf animals, on the other hand, were monitored for activity 1 day prior to the timepoints at which they were scanned.

Each activity monitoring lasted 24-hours to account for day and night activity patterns, with measurements recorded in 30-minute intervals (i.e. 48 measurements per session). IR beam spacing was at a constant of 1.5” at a wavelength of 875nm and 160Hz beam scan rate.

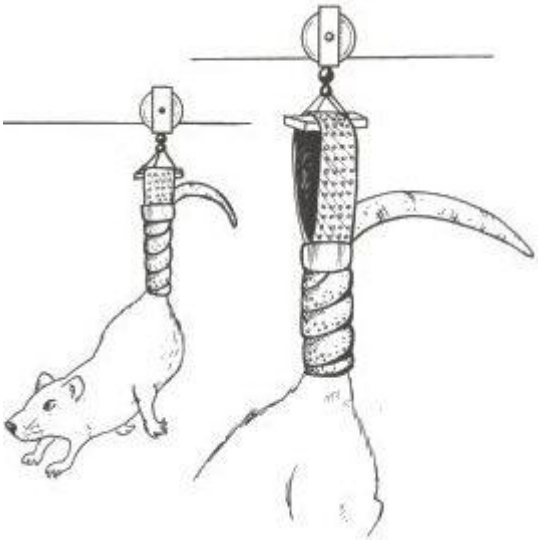

Figure 3. **Schematic diagram of hindlimb unloading procedure used to create a disuse environment for rodents. Mice are fitted with a tail harness that used to suspend their caudal skeleton from an overhead beam. The mice can ambulate within the cage by using their forelimbs, which remain in contact with the cage floor, to slide the tail harness along the overhead beam. (Image Courtesy: http://www.nsbri.org/HumanPhysSpace/focus5/f5-221.html)**

3.4 HINDLIMB SUSPENSION

HLU was effected by the Morey-Holton rodent suspension model. (Fig. 3) [57] Disuse was effected via tail suspension of the mice (under anesthesia over the course of the procedure of suspending them). This simulates cephalic fluid-shift among other critical physiological consequences of microgravity.

3.5 ANIMAL CARE FOR ANIMALS IN SUSPENSION

Experimental group animals, over the course of HLU, were single-housed in standard rat cages with *ad libitum* access to water and food (rodent chow, dry treats such as cereals, fruity gems, napa nectar, and peanut butter). Dry treats helped maintain mouse appetite and controlled their weight loss to a significant extent. The animals were monitored daily to ensure good health, and secure and non-infectious suspension. Criteria included animal weight, urination/ defecation, eye goop, presence/ absence of blood etc. Animals that exhibited a weight loss of more than 30% from day 0 of suspension for more than 4 days consecutively were removed from the experiment, for health concerns. Stark weight losses of more than 2 grams for the previous day was handled by administering subcutaneously administering Lactate Ringers' solution.

Figure 4. Transverse view of microCT prior to scanning showing the positioning of mice femur for femoral scan.

3.6 IN VIVO MICRO-COMPUTED TOMOGRAPHY (MICROCT)

As mentioned earlier, the 3wf and 9wf groups were scanned *in vivo* prior to and post their HLU durations, while the cf group was scanned at the 6 timepoints mentioned in Fig. , to ensure an equal total exposure to radiation throughout all groups across the duration of the experiment. Earlier studies have proven this to be optimal exposure, considering that the micro-CT only exposes the volume of interest (VOI) to radiation, and not surrounding tissues.

Animals were anesthetized with isofluorane and scanned by means of micro-computed tomography at the timepoints mentioned earlier. (VivaCT 75, Scanco Medical Inc., SUI 45kV, 300-ms integration time, 512x512 pixel matrix, 156 micron isotropic voxel size). The MicroCT allows quantification of bone morphology and architecture longitudinally, thus making it a powerful modality.[125]

3.6.1 Fat Scan

Each animal was placed on the cradle (/ gantry) with its abdomen facing upward, and taped across the chest to prevent motion artifact. The abdomen was scanned at 105mAs for 265 slices at a 76µm resolution, with the region of interest (ROI) from the pelvic area to the rib cage transversely. The landmarks were set from the proximal end of L1 vertebra to the distal end of L5 vertebra. Abdominal tissue was quantified in terms of visceral, subcutaneous, and total abdominal tissue fat (VAT, SAT, TAT respectively), lean tissue mass (LTM), apparent vertebral bone mineral density (aVMD), and vertebral bone volume (BoneV), using a customized image processing script.[126, 127]

3.6.2 Femur Scan

Each fat scan was followed by a femur scan (Fig. 4) with the ROI selected from the femoral growth plate to the midshaft via a transverse scout view window, at 166mAs spanning 424 slices. The CT images were processed using specific algorithms developed[128] to analyze the distal metaphysis and mid-diaphysis, and extract parameters defining trabecular and cortical bone morphology:

1. Bone volume (BV) and bone volume fraction (BV/TV),
2. Trabecular number (Tb. N), thickness (Tb. Th) and spacing (Tb. Sp),
3. Cortical thickness (Ct. Th) and area (Ct. Ar),
4. Trabecular and cortical apparent and tissue mineral densities (Tb. AMD, Tb. TMD, Ct. AMD, Ct. TMD),
5. Endosteal and periosteal volume(Endo. V and Peri. V), surface (Endo. S and Peri. S), and envelop (Endo. Env and Peri. Env), and
6. Moments of Inertia – principal (pMOI), maximum (Imax) and minimum (Imin).

3.7 FINITE ELEMENT MODELING (FEM)

Segmented AIM files of the distal metaphysis of the femur (Fig. 17(a)(i) and Fig. 17(b)(i)) were subjected to a uniaxial stress compression test in the z-direction simulated using IPL ScancoFE, Version 1.13 (Scanco Medical, Switzerland). The samples were oriented with the proximal and distal surfaces along the xy-plane, such that a 1N compression was uniformly applied in a transverse fashion without

friction.[110] The FE model was generated via a 2-step iterative FE-solver system[129] that generates a nodal mesh structure and equations at each node in the pre-processing stage, and then computing mechanical parameters relevant to the user-given problem statement by injecting values into the equations. The pre-set values input for this experiment were force (N) and displacement (mm) tolerances of 1×10^{-4}, trabecular and cortical elastic modulii (E) of 25GPa and Poisson's ratio 0.3.[130-132] Von-Mises stresses were calculated for all elements, for whole bone as well as individually for the cortex and trabeculae (Fig. 17(a)(ii) and Fig. 17(b)(ii)). The 95^{th} percentile was chosen as Peak Von-Mises equivalent stress (PVM) (in MPa) in order to downplay artifacts and singularities.[110] The median value was also chosen for representation, to give a fair idea of the disparity in stress distribution.

3.8 COMPUTATIONAL ANALYSIS

All values are presented as mean+SD. Correlation was calculated eventually between the morphological and mechanical indices by estimating squares of Pearson correlation coefficients between group-wise TOT activity counts and corresponding time-matched indices. This was then multiplied by 100 to derive percentage estimates.

4. RESULTS

4.1 ACTIVITY MONITORING

4.1.1 Baseline Activity Pattern

Total activity count over a 24-hour period at baseline across all groups (cf, 3wf, and 9wf), demonstrated that z TOT, xy AMB, and xy TOT maintained the same proportions. (Fig. 5)

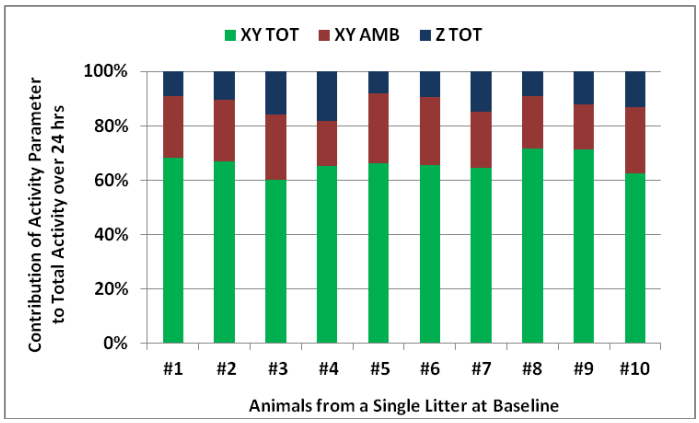

Figure 6. Baseline 24h activity patterns of 10 F2 mice at baseline showing a high level of similarity among them. Z TOT = total activity in the z direction, XY AMB = ambulatory activity in the xy plane, XY TOT = total activity in the xy plane.

Since this showed that the ratios of individual activity measurements, themselves, were not significantly different from each other, from this point further, activity is taken to be a single value which is the sum of these 3 parameters(, i.e. z TOT + xy AMB + xy TOT). Also, the experimental design does not affect/ concern the day/ night activity patterns, each activity timepoint for an animal is accounted for as the average of total activity counts (z TOT + xy AMB + xy TOT) over the 48 intervals in each session.

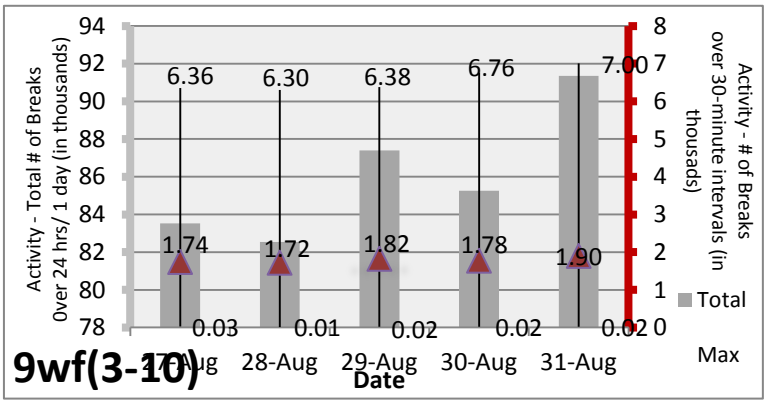

Figure 5(a). Total and average activity of an 8 F2 mice litter comparing average activity levels on 5 consecutive days (08/27/2011 to 08/31/2011) after release from the first cycle of suspension.

4.1.2 Activity Pattern over First Week of Reambulation

As a pilot study to observe the activity immediately after release from suspensions, the 9wf(3-10) litter was activity monitored for the first 5 consecutive days of RA1, immediately after relase from HLU1 on the 26th of August, 2010. The motivation behind this being that on return to RA after 3 wks in suspension, there is a need for the animal to acclimatise to the sudden change in loading state and physiology. Hence the speculation that activity measurement on the first day of RA might perhaps not truly gauge the animal activity purely owing to its unloading state needed verification.

The total activity per day, average activity per day, and maximum and minimum activity values recorded in a day were studied. Day 3 consistently served as a point of symmetry for all the animals (Fig. 6(b)) as indicated by the average litter plot (Fig. 6(a)), with the activity before it reflecting severe fluctuation (possibly attributed to the sudden change in loading state), stabilizing over day 4 (in terms of activity values and variance), and spiking up on day 5 (perhaps with the effect of RA beginning to set in). With this, it was decided that the most apt portrayal of the effect of HLU could be obtained by recording activity on the 4^{th} day of RA.

4.1.3 Individual Activity

4.1.3.1 *cf Group*

The average activity at baseline (16wks) started off between 1500 – 3600 counts, and went on to dip slightly after 3 wks (at 19wks), activity coming down to 1000 – 2500 counts. Interestingly, the percentage loss over these 3wks was about the same across the 4 animals, with cf1, cf2, and cf3 losing a nearly uniform 30%, and cf4 slightly more at 50% loss. This reduce in activity carried on to the next timepoint at 28wks, however at a much lesser slope. cf2 dipped lowest to 720 counts here, around which cf3 and cf4 hovered, while cf1 is at a high 1600 counts. cf3 dropped only 17% from its 19wk activity level, but the others lost about 30%. However, from baseline, all 4 mice lost about an equal 50-60% from baseline.

The next 3wks from here, 31wks, was the first point where activity trends were a bit different, with a near inversion pushing cf1 lowest (370) in average activity and cf2 most active (970). While this was a 34% gain from 28wks and only a 30% loss from baseline, cf1 suffered 78% and 90% losses from 28wks and 16wks respectively. The sixth and final point for monitoring the activity for the cf animals at 40wks, corresponded to the release of 9wf from its third and last HLU exposure, brought about a spur in activity again (1000 – 1500 counts). With cf1 having been most active except for the 31wk point where it took an uncharacteristic down-swing, this rise at 40wks was an incredible 300% from the 31wk trough stabilizing the loss from baseline at 60%. cf2, on the other end, experienced as less as a 10% gain from 31wks while losing only a fourth from baseline. (Fig. 7(a))

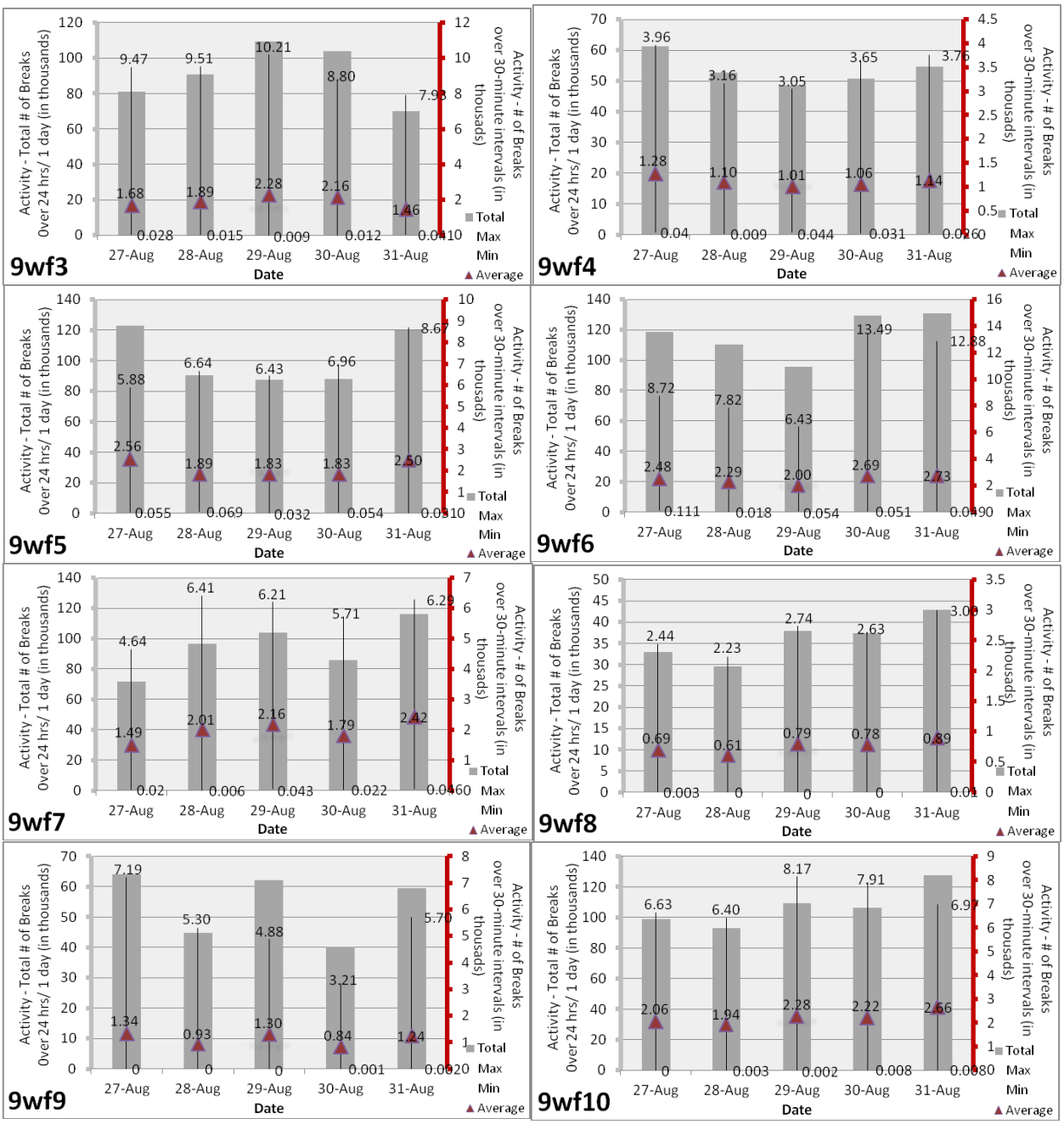

Figure 6(b): Total and average activity of 8 F2 mice portrayed individually, comparing average activity levels on 5 consecutive days (08/27/2011 to 08/31/2011) after release from the first cycle of suspension.

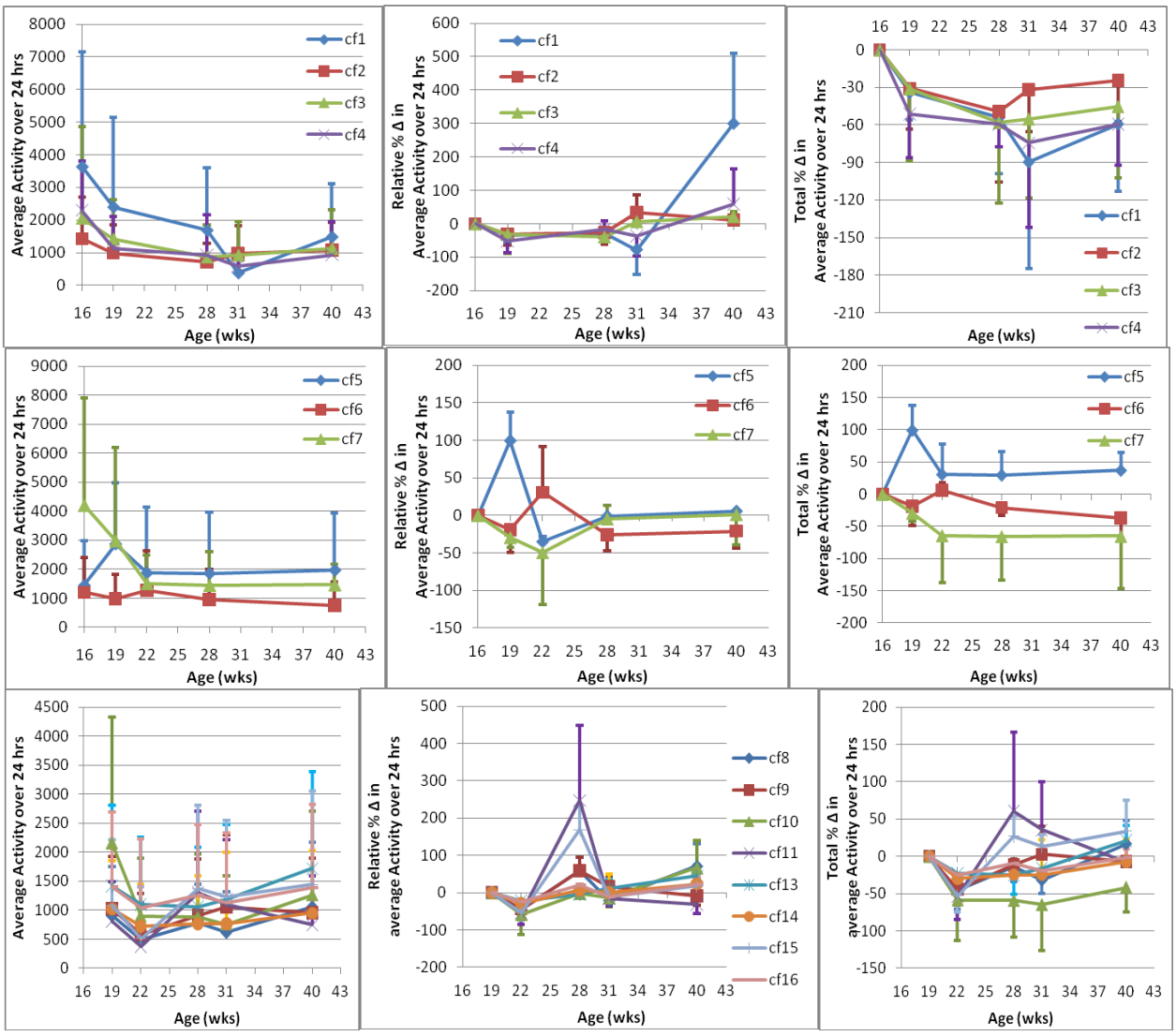

Figure 7(a): Average activities of individual animals that comprise the 3 litters of control (cf) mice: cf(1-4), cf(5-7), and cf(8-16) expressed as absolute mean values of activity averaged across 24hrs, relative percentage changes in average activity where each time point is compared with the previous time point of measurement, and total percentage change representing the percentage of change of activity at each timepoint with respect to corresponding baseline activities (at 16wks). All values are expressed as mean+SD.

Revisiting primary observations, it can now be said that cf1 was most active overall and cf2, the least; but cf1's activity fluctuated most through this 16wk to 40wk time period, while cf3 was least sensitive to ageing and other activity-governing factors. The second litter of 3 mice, cf(5-7), though similar for the most part, had a slightly different twist, with a fairly linear drop in activity through the 1st 6 weeks, and plateauing thereafter. cf7 was the highest responder upto 19wks after which activity values were not significantly different compared to cf5 and cf6, the latter of which being the least active and least fluctuating of the litter. Baseline average activity was 4000 for cf7 while cf5 and cf6 were around 1300

counts. Interestingly enough, 3wks from baseline, a 30% decrease in cf7 activity was met by a doubling of cf5 activity, both averaging in activity at 3000 counts. cf6 however drops by 20% to a 1000. In another 3wks, both cf5 and cf7 became less reactive, coming in the vicinity of cf6 activity that experienced a small but insignificant increase. The percentages changes here were interesting, cf7 going down by another 50% in the 19-21wk interval as it did over the previous 3wk gap, cf5 and cf6 losing and gaining about 32.5% respectively from 19wk activity states, while cf7 losing a little more than double its activity (65%) as cf5 (30%) from baseline. For the rest of the 18wks, cf5 and cf7 maintained their activity levels while cf6 lost a fourth of its activity at 28wks and thereafter joined cf5 and cf7's stable activity pattern compared to the 22wk point. Owing to the contrast between activity levels versus fluctuation in activity, cf5 and cf6 stood to gain and lose 35% while cf7 lost more than double its high activity start (65%) from baseline at the 40wk point of conclusion.

The last of the controls consisted of 8 mice - (cf(8-16), (except for cf12 that died at baseline). Baseline activity lied around 800 – 1000 counts, with the outliers being cf10 – as active as 2100 average movements per 30 minutes over the 24-hour period of observation – and cf13 and cf16 at 1400 counts. In a matter of just 3wks, the litter came down to a uniform average activity ranging between 300 and 1100 counts, dropping between a fourth and half in its activeness. There was a general increase over the following 6wks (22-28wks of age), with activity at 800 – 1400 counts, the largest raises being experienced by cf11 (2.5 times as active as 22wks and 0.6 times as baseline) and cf15 (1.5 times as active as 22wks and 0.25 times as baseline), while the rest of the litter gained anywhere between 0 – 0.6 times and -0.6 – 0.6 times from the 28wks and 16wks levels respectively. 31wk activity levels decreased from 28wks on a very minimal scale (average of 600 – 1200 counts).

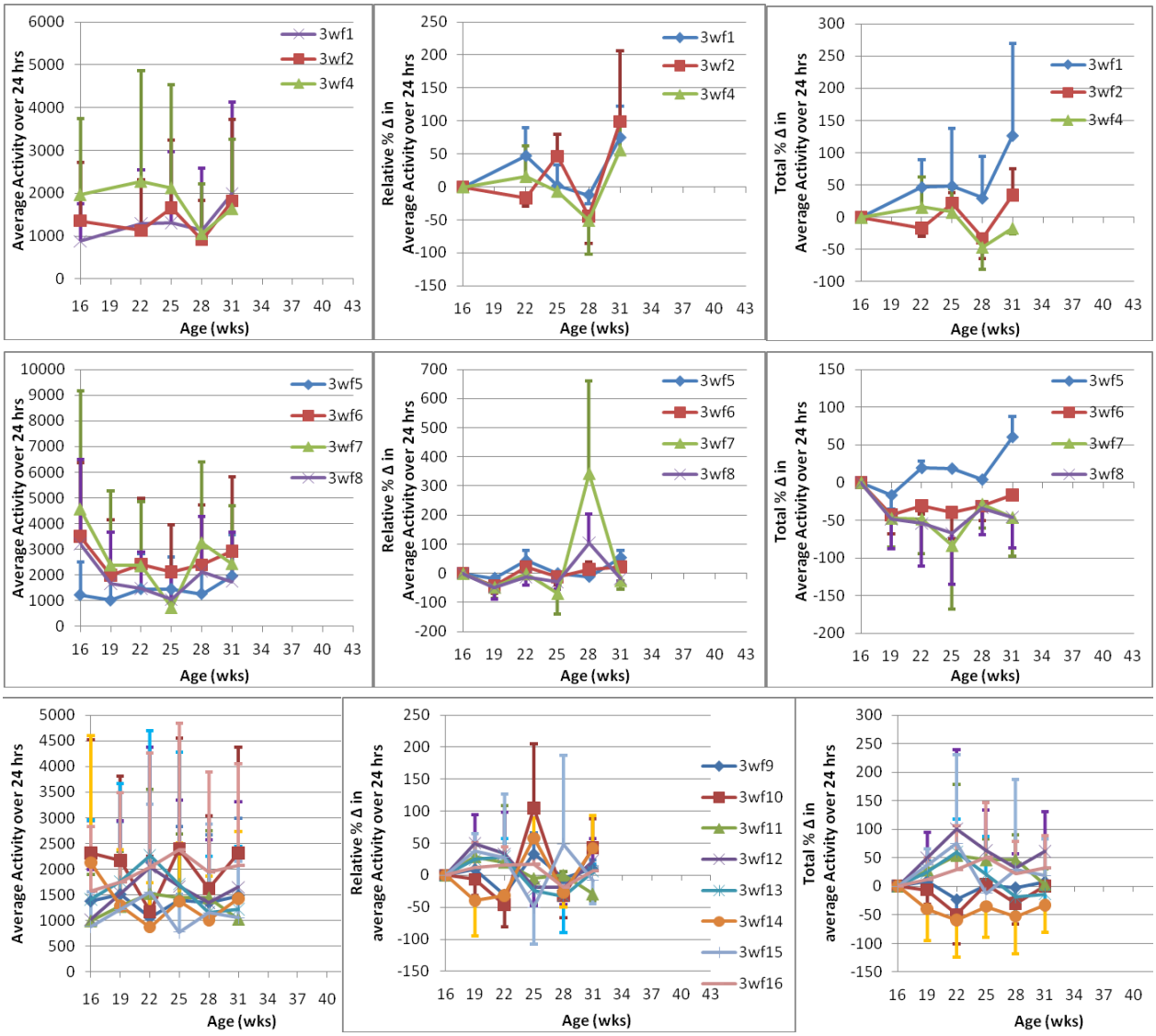

Figure 7(b): Average activities of individual animals that comprise the 3 litters of 3wf experimental group mice: 3wf(1-4), 3wf(5-8), and 3wf(9-16) expressed as absolute mean values of activity averaged across 24hrs, relative percentage changes in average activity where each time point is compared with the previous time point of measurement, and total percentage change representing the percentage of change of activity at each timepoint with respect to corresponding baseline activities (at 16wks). All values are expressed as mean+SD.

But from the 40wk standpoint, there was a linear slope of decrease from 28wks through 31wks to 40wks, pitching anywhere between 700 and 1700 average counts. Gains from 31wks figured at 20% – 45% and 8% – 33% losses from baseline, with the outliers being cf8 losing 10% from 31wks and cf9 gaining nearly 70% from 31wks and losing 40% from baseline. This said, this 8-mouse litter presented a rather complex relationship in activity. cf11 was perhaps most active, closely followed by cf15; cf10 and

cf16 bridged the other end of the spectrum. These 2 sets were also most and least fluctuating respectively.

4.1.3.2 *3wf Group* (Fig. 7(b))

4.1.3.3 *9wf Group* (Fig. 7(c))

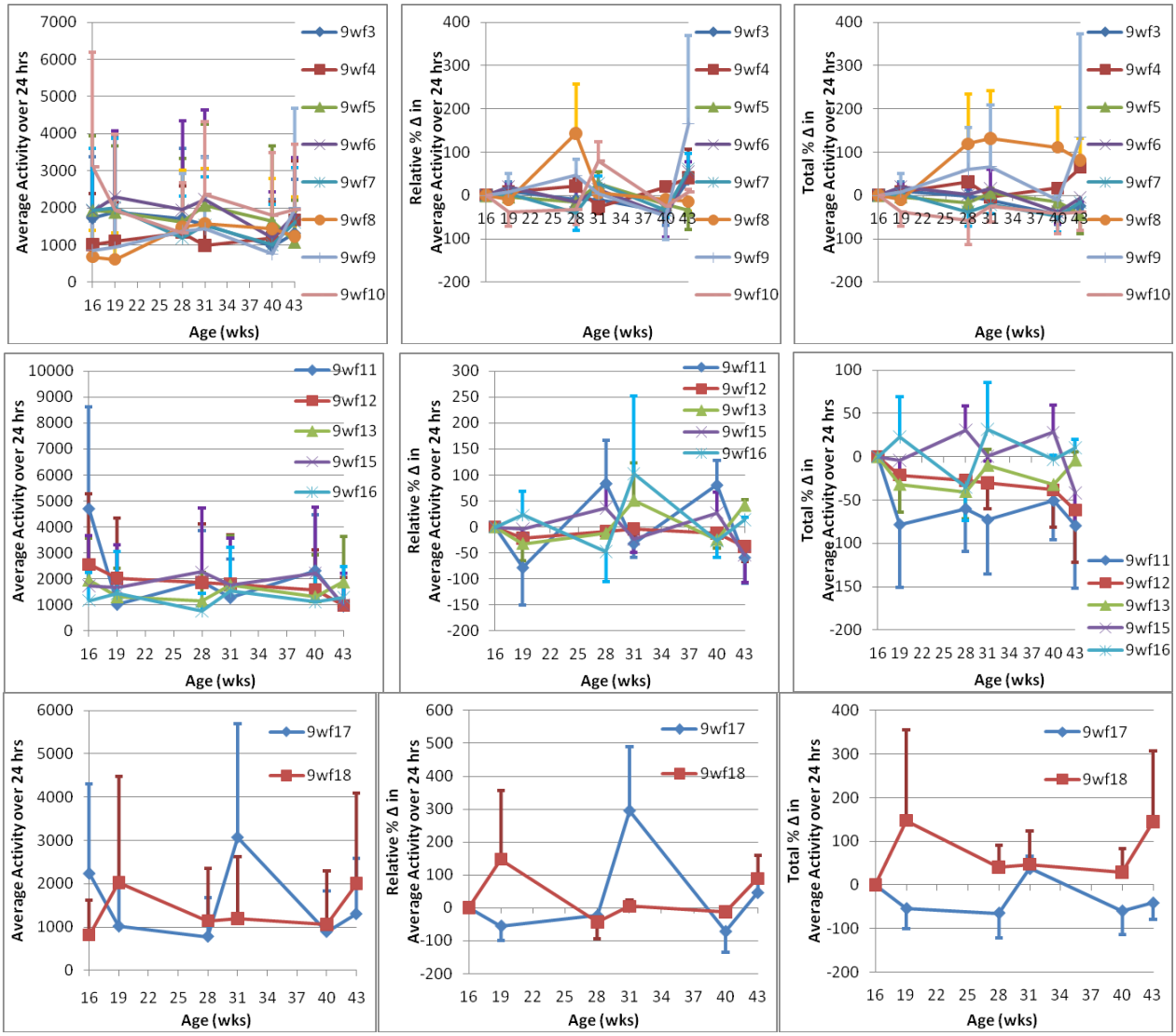

Figure 7(c): Average activities of individual animals that comprise the 3 litters of 9wf experimental group mice: 9wf(3-10), 9wf(11-16), and 9wf(17-18) expressed as absolute mean values of activity averaged across 24hrs, relative percentage changes in average activity where each time point is compared with the previous time point of measurement, and total percentage change representing the percentage of change of activity at each timepoint with respect to corresponding baseline activities (at 16wks). All values are expressed as mean+SD.

4.1.4 Litter-Based Activity

4.1.4.1 *cf Group*

The third litter experienced a sudden doubling in activity between 22 and 31wks, upto which point the first 2 litters experienced a gradual decline in activity upto 50%. But the 1st litter faced a doubling in activity from 31wks to 40wks over which the other 2 were fairly stable. Consequently, at the 40wk endpoint, litters were comparable in activity (Fig. 8(a)), varying in magnitude by atleast 20% from each other.

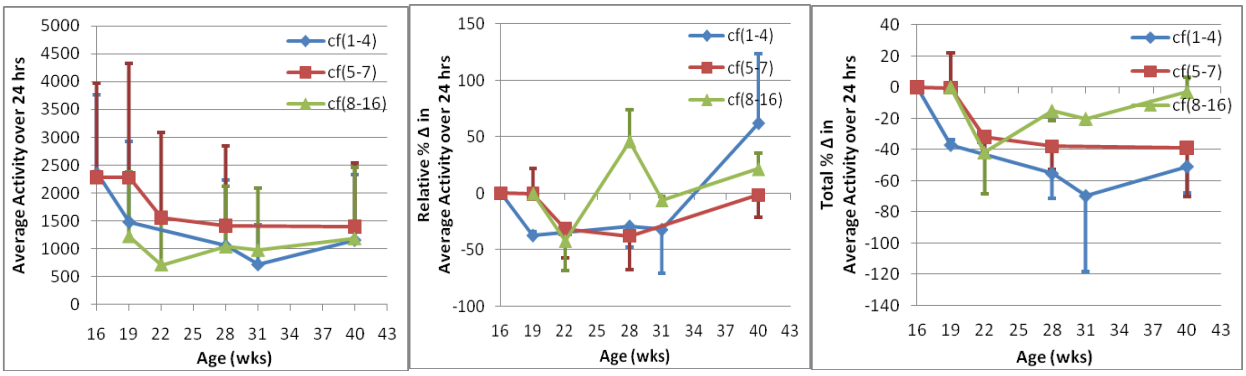

Figure 8(a): Average activities of the 3 litters of control (cf) mice: cf(1-4), cf(5-7), and cf(8-16) expressed as absolute mean values of activity averaged across 24hrs, relative percentage changes in average activity where each time point is compared with the previous time point of measurement, and total percentage change representing the percentage of change of activity at each timepoint with respect to corresponding baseline activities (at 16wks). All values are expressed as mean+SD.

4.1.4.2 *3wf Group*

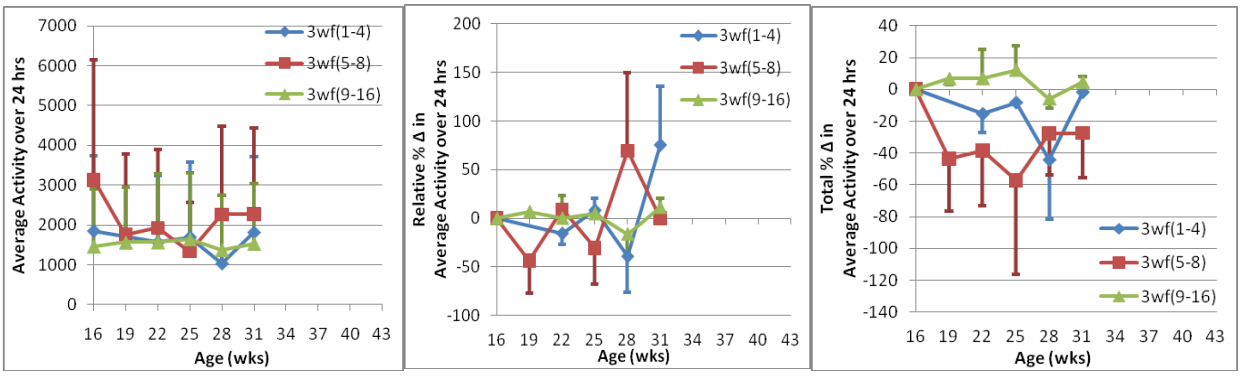

Figure 8(b): Average activities of the 3 litters of 3wf mice: 3wf(1-4), 3wf(5-8), and 3wf(9-16) expressed as absolute mean values of activity averaged across 24hrs, relative percentage changes in average activity where each time point is compared with the previous time point of measurement, and total percentage change representing the percentage of change of activity at each timepoint with respect to corresponding baseline activities (at 16wks). All values are expressed as mean+SD.

While the first litter was deviant, the activity dropped by a mere 300 counts over 6wks (HLU1 and RA1). After HLU2 activity rose by 100. RA2 and HLU3 then brought about a drop of 600 average breaks and shoot of 800 respectively. At the end of the 15wks of experiment, the 1st and 3rd litters (11 of 15 mice) had an activity similar to baseline values. The 4 others were about 30% less active than baseline.(Fig. 8(b))

4.1.4.3 *9wf Group*

The first litter fell short of prior activity by 250 counts after RA2 but nearly recovered it over HLU3. The second group of 5 mice were significantly less active after HLU1 and HLU3, otherwise almost invariant, with the slightest increment over the 19wk – 40wk duration. Relative changes reconfirmed this with a change of ±30% over any interval across the litters. (Fig. 8(c))

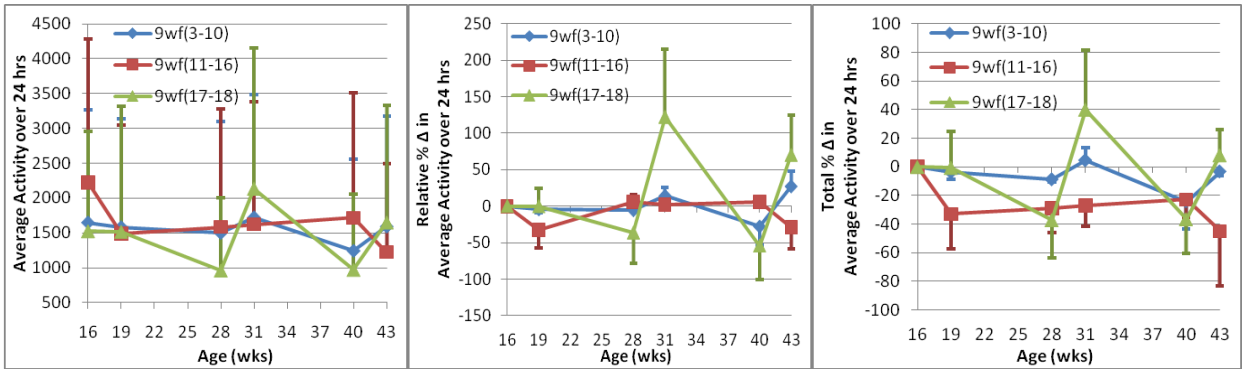

Figure 8(c): Average activities of the 3 litters of 3wf mice: 9wf(3-10), 9wf(11-16), and 9wf(17-18) expressed as absolute mean values of activity averaged across 24hrs, relative percentage changes in average activity where each time point is compared with the previous time point of measurement, and total percentage change representing the percentage of change of activity at each timepoint with respect to corresponding baseline activities (at 16wks). All values are expressed as mean+SD.

4.1.5 Group-Based Activity

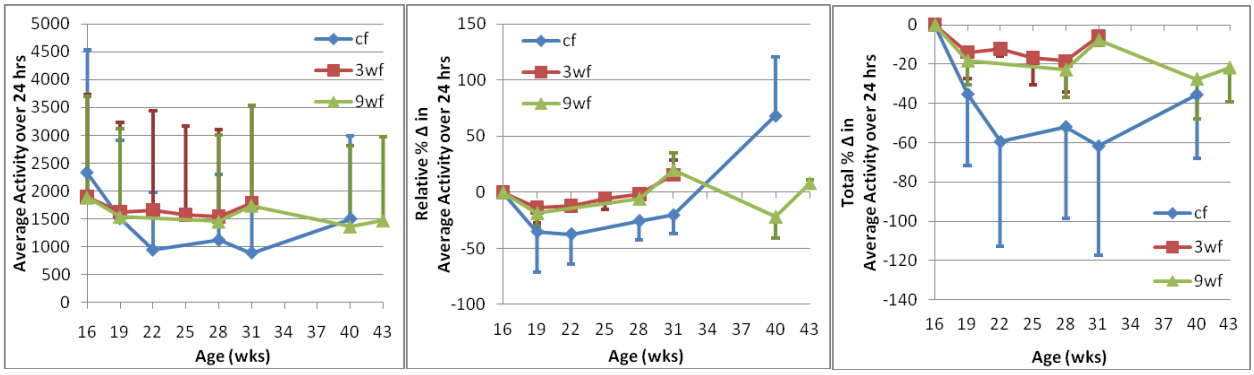

Figure 9. Average activities of the control group (cf) and experimental groups: 3wf and 9wf, expressed as absolute mean values of activity averaged across 24hrs, relative percentage changes in average activity where each time point is compared with the previous time point of measurement, and total percentage change representing the percentage of change of activity at each timepoint with respect to corresponding baseline activities (at 16wks). All values are expressed as mean+SD.

The absolute mean activity was within 500 counts for 3wf and 9wf, and varied upto 1100 for cf. Subsequent-interval and from-baseline percentage changes were within ±20% and -20% respectively for experimental groups, and as much as (-40%–60%) and -60% respectively for controls. (Fig. 9)

4.2 MORPHOLOGY

4.2.1 Abdominal Fat and Lumbar Spine

Owing to a high standard deviation, TAT normalized over LTM portrayed a better estimate of true volume variations. (Fig. 10)

4.2.2 Femur

4.4.2.1 *Distal Metaphysis*

a) Volumetric Variations

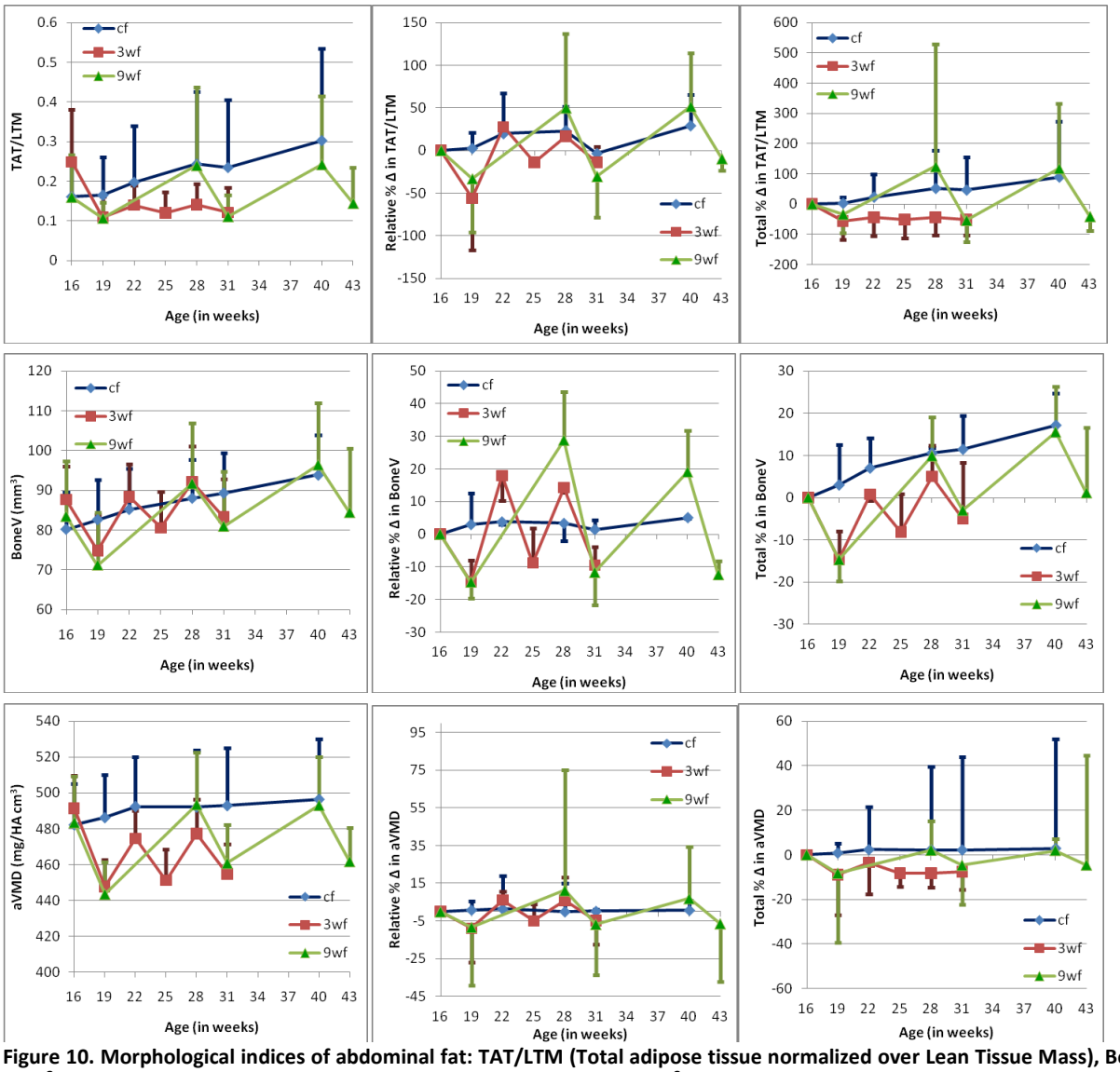

Figure 10. Morphological indices of abdominal fat: TAT/LTM (Total adipose tissue normalized over Lean Tissue Mass), BoneV [mm^3] (volume of bone in the lumbar spine), and aVMD [mg/HA-cm^3] (apparent volumetric mineral density) compared across the control (cf) and experimental (3wf, 9wf) groups in terms of mean values, relative percentage changes over subsequent timepoints, and total percentage change in value from baseline (16wks). All values are expressed as Mean+SD.

Trabecular BV/TV stabilized beyond 31wks while cortical BV/TV continued degrading. 3wf sloped down to over -35% at 19wks and then a gradual -45% at 28wks and is at -50% at 31wks. (Fig. 11(a))

On the other hand, 9wf jumped a nearly similar -30% at 19wks, (reconfirming the comparability of groups over the same exposure to disuse) recovering up to -20% from baseline at 28wks and closing at -45% at 43wks. Ct. BV/TV on the other hand, had cf at -0.2% at 19wks, -1% at 28wks, and -2.7% at 40wks; 3wf at -2.6% at 19wks with respect to baseline, -0.4% at 28wks, and a -2.8% at 31wks post HLU3; 9wf at -2% at 19wks, -0.3% at 28wks, and -6.8% at 40wks.

b) Properties of Trabeculae

Tb. Th increased from 0.0723mm at baseline to 0.0825mm at 40wks for cf. 3wf was 14% higher than its baseline Tb. Th at 31wks, at which point cf was 11%, In contrast, 9wf was at 13% Tb. Th at 40wks from 16wks, while cf was 32% at the same age. (Fig. 11(b))

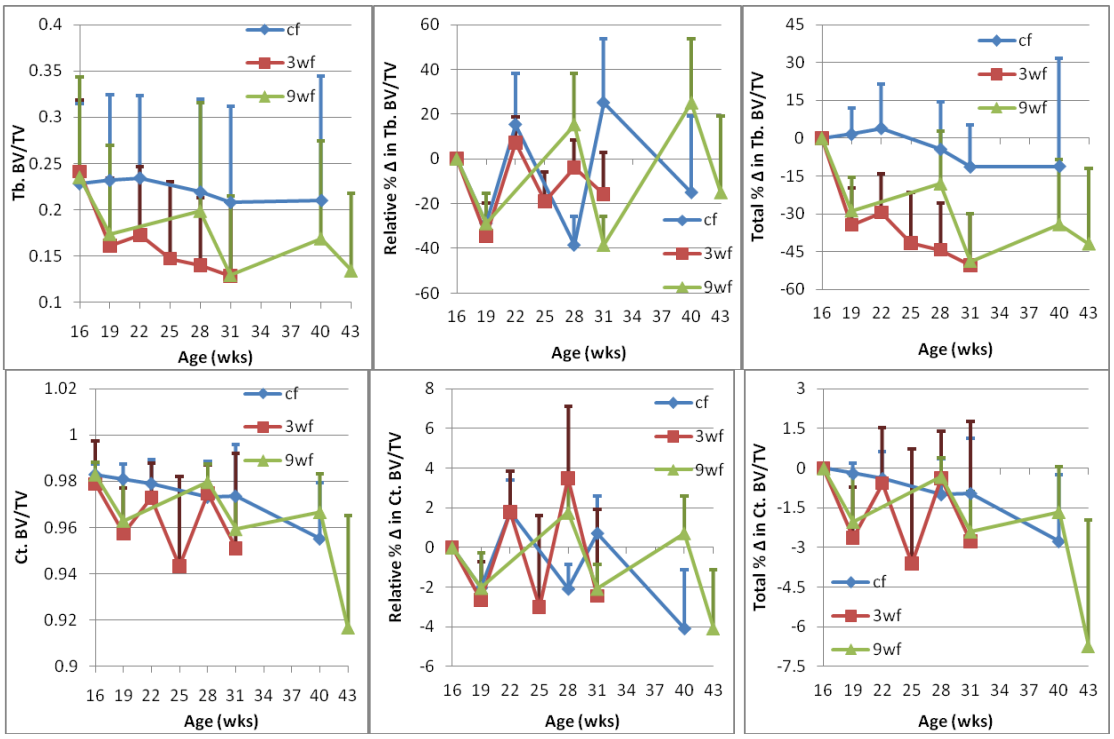

Figure 11(a): Volumetric morphological indices of the femoral distal metaphysis: Tb. BV/TV and Ct. BV/TV (Trabecular and Cortical Bone Volume fractions respectively) compared across the control (cf) and experimental (3wf, 9wf) groups in terms of mean values, relative percentage changes over subsequent timepoints, and total percentage change in value from baseline (16wks). All values are expressed as Mean+SD.

c) Density Comparisons (Fig. 11(c))

Tb. AMD for cf went down by 25 mg/HA-cm^3 (7.5%) over 24wks while 9wf lost as much as 50 mg/HA-cm^3 over the same duration (during which it experienced 2 cycles of HLU and RA) (20% loss). In a 15wk

period from start, where cf had lost about just the same of 25 mg/HA-cm^3, 3wf dropped by a little more than 30% (100 mg/HA-cm^3) from baseline after going through 3 periods of HLU and 2 RAs. Ct. AMD on the other hand, reduced by 20 mg/HA-cm^3 (2%) over 24wks for cf, over which 9wf lost less, though not significantly so – 15 mg/HA-cm^3! Likewise, when cf gained cortical density of 10 mg/HA-cm^3 (0.75%), 3wf stood to lose 30 mg/HA-cm^3 (3%). 3wf over 31wks (, 3 HLUs and 2 RAs in between,) experienced 10% greater loss than 9wf (over just 2 cycles of HLUs and RAs). On the other hand, trabecular and cortical compartments experienced TMD variation within ±2% through the experiment for controls and experimental groups.

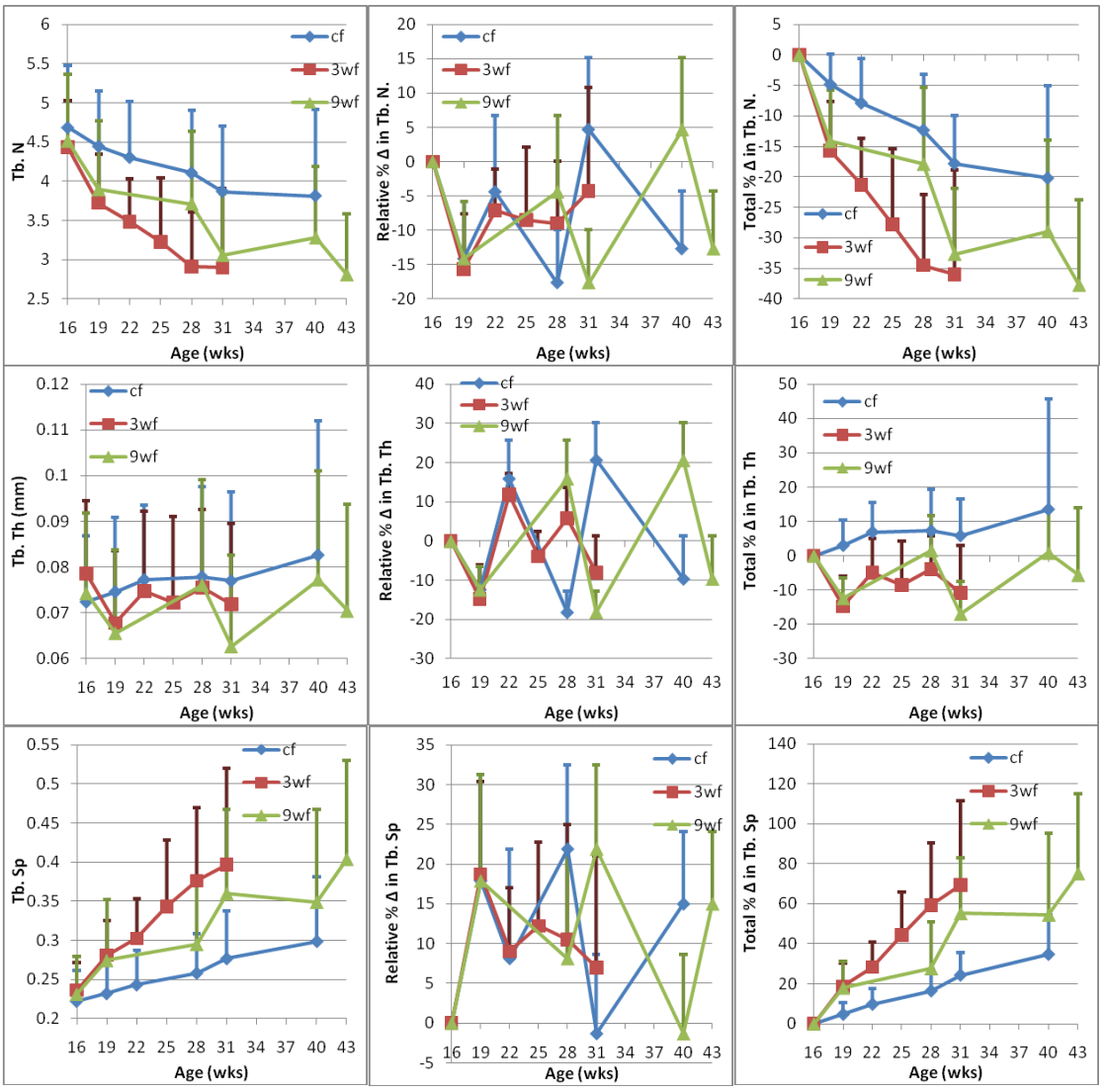

Figure 11(b): Typifying morphological indices of the trabecular compartment of the femoral distal metaphysis: Tb. N, Tb. Th [mm], and Tb. Sp (Trabecular Number, Thickness, and Spacing respectively) compared across the control (cf) and experimental (3wf, 9wf) groups in terms of mean values, relative percentage changes over subsequent timepoints, and total percentage change in value from baseline (16wks). All values are expressed as Mean+SD.

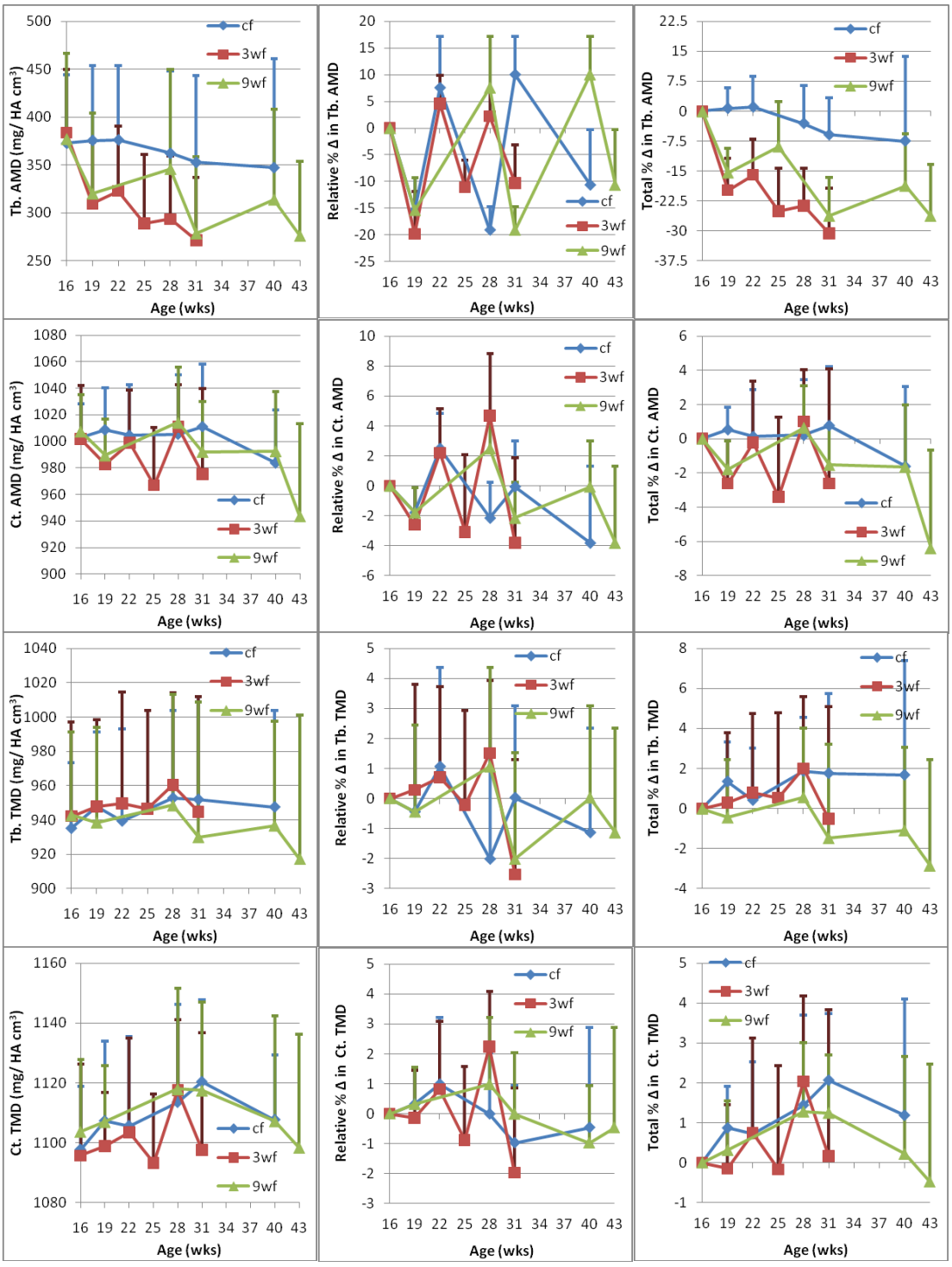

Figure 11(c): Quantifications of density-based indices of the femoral distal metaphysis: Tb. AMD and Ct. AMD, Tb. TMD and Ct. TMD, all [mg/HA-cm^3] (Trabecular and Cortical apparent and tissue mineral densities respectively) compared across the control (cf) and experimental (3wf, 9wf) groups in terms of mean values, relative percentage changes over subsequent timepoints, and total percentage change in value from baseline (16wks). All values are expressed as Mean+SD.

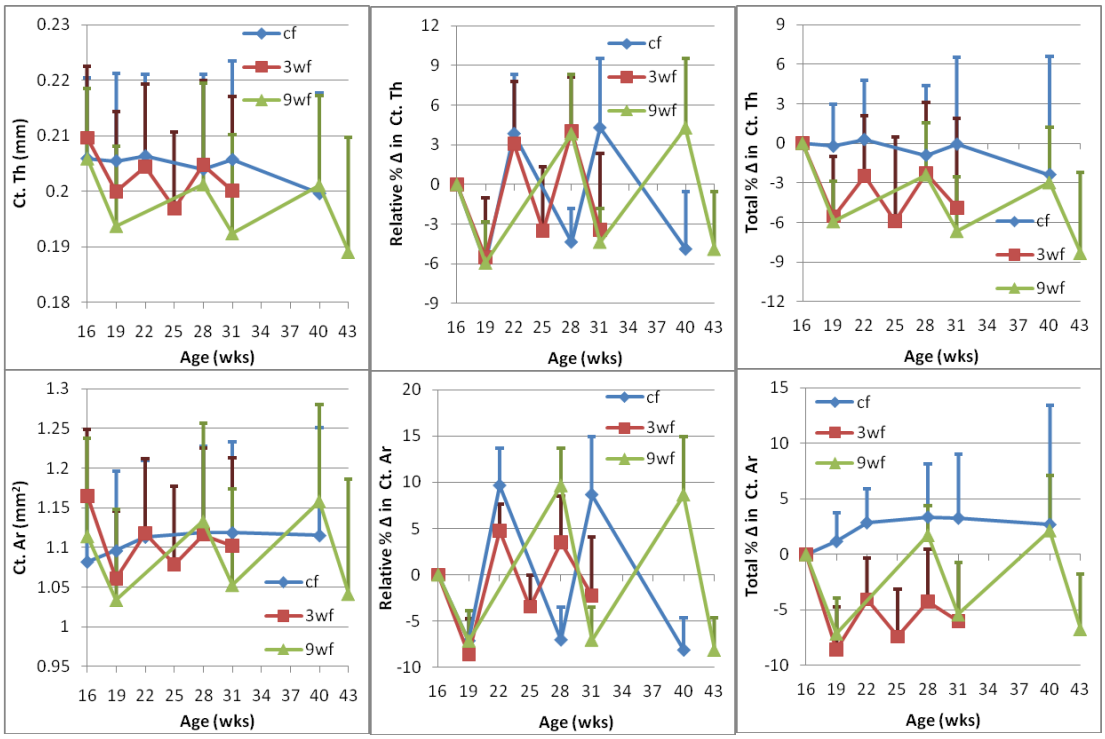

Figure 11(d): Typifying morphological indices of the cortical compartment of the femoral distal metaphysis: Ct. Th [mm] and Ct. Ar [mm^2] (Cortical Thickness and Area respectively) compared across the control (cf) and experimental (3wf, 9wf) groups in terms of mean values, relative percentage changes over subsequent timepoints, and total percentage change in value from baseline (16wks). All values are expressed as Mean+SD.

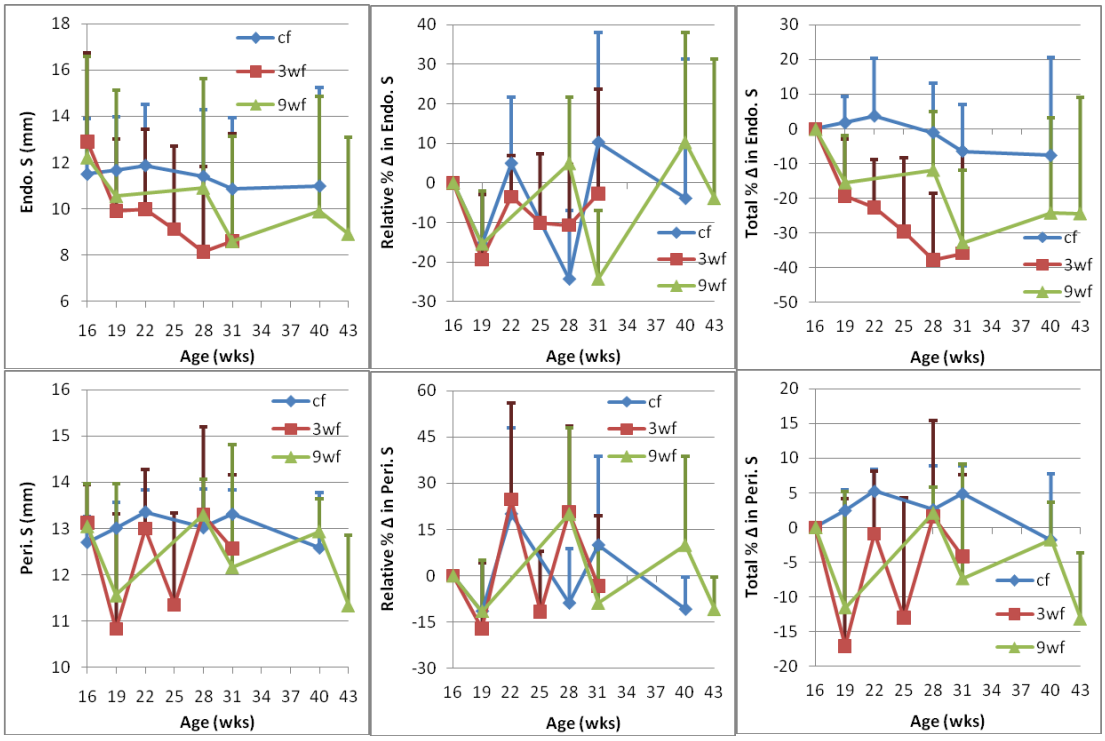

Figure 11(e)(i): Morphological measures of the surface of the femoral distal metaphysis: Endo. S [mm] and Peri. S [mm] (Endosteal and Periosteal Surface lengths respectively) compared across the control (cf) and experimental (3wf, 9wf) groups in terms of mean values, relative percentage changes over subsequent timepoints, and total percentage change in value from baseline (16wks). All values are expressed as Mean+SD.

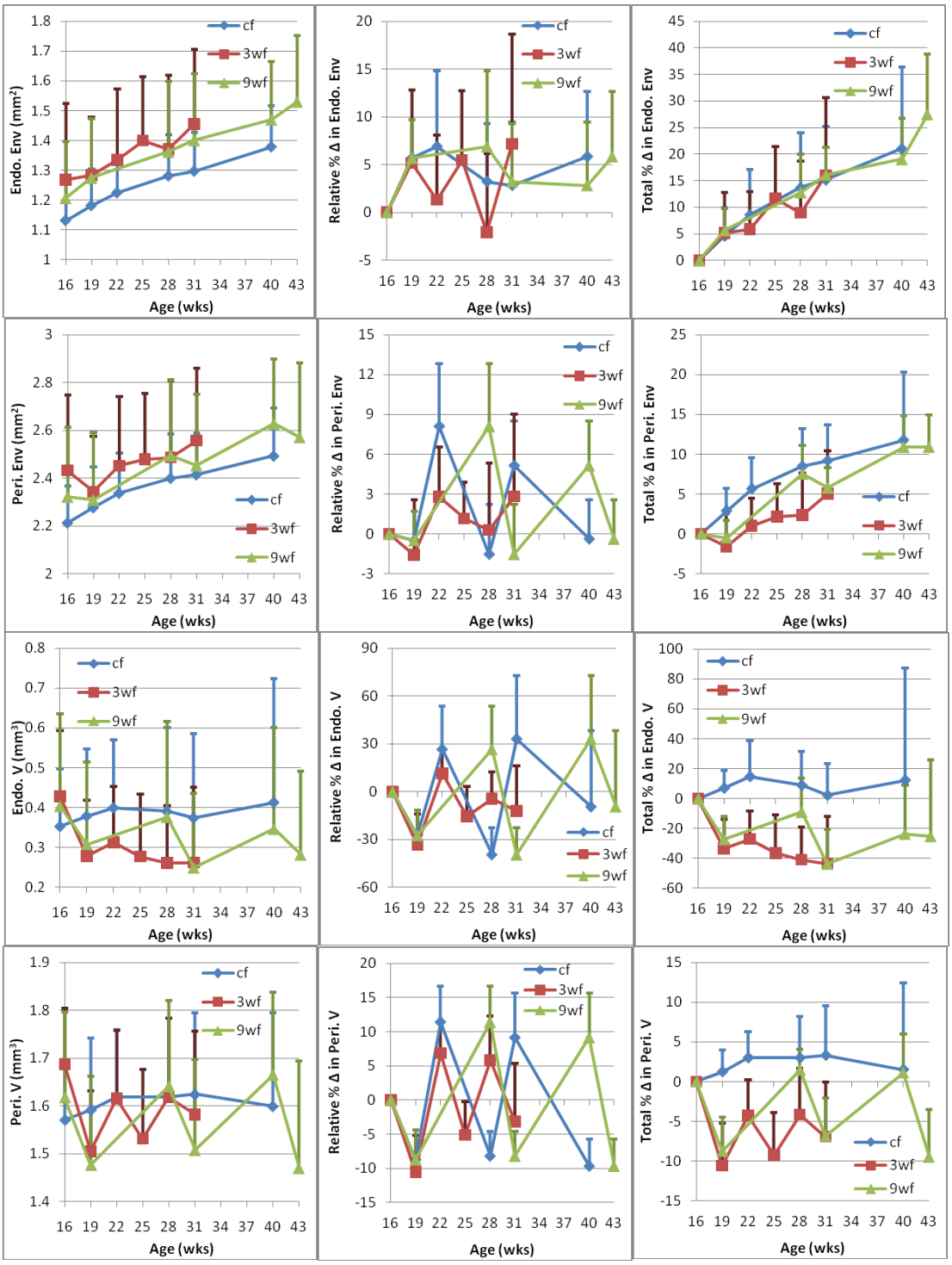

Figure 11(e)(ii): Morphological measures of the surface of the femoral distal metaphysis: Endo. Env and Peri. Env, [mm^2], Endo. V and Peri. V, [mm^3], (Endosteal and Periosteal Envelop area and volumes respectively) compared across the control (cf) and experimental (3wf, 9wf) groups in terms of mean values, relative percentage changes over subsequent timepoints, and total percentage change in value from baseline (16wks). All values are expressed as Mean+SD.

d) Properties of the Cortex (Fig. 11(d))

Tb. Th dropped by 10% from baseline for 3wf at 31wks while Ct. Th changed by a downswing of only 5%. Tb. Th for 9wf, in contrast, came down by 7.5% over 43wks, and Ct. Th by nearly 9%.

e) Surface Indices

Periosteal reduction in surface limited itself within 20% while endosteal surface loss scaled upto 40%, both for the 3wf. 9wf losses were within 15% and 30% respectively. (Fig. 11(e)(i)) This ratio of proportionality reflected in envelop and volume measures. (Fig. 11(e)(ii))

f) Moment of Inertia (Fig. 11(f))

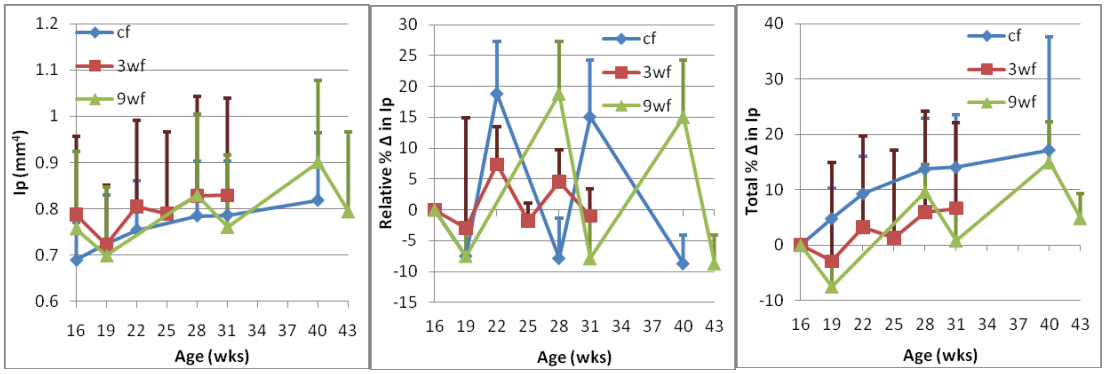

Figure 11(f): Inertial quantification of the femoral distal metaphysis: Ip[mm^4] (Principal Moment of Inertia) compared across the control (cf) and experimental (3wf, 9wf) groups in terms of mean values, relative percentage changes over subsequent timepoints, and total percentage change in value from baseline (16wks). All values are expressed as Mean+SD.

4.4.2.2 *Mid-Diaphysis*

a) Properties of the Cortex (Fig. 12(a)(i), 12(a)(ii))

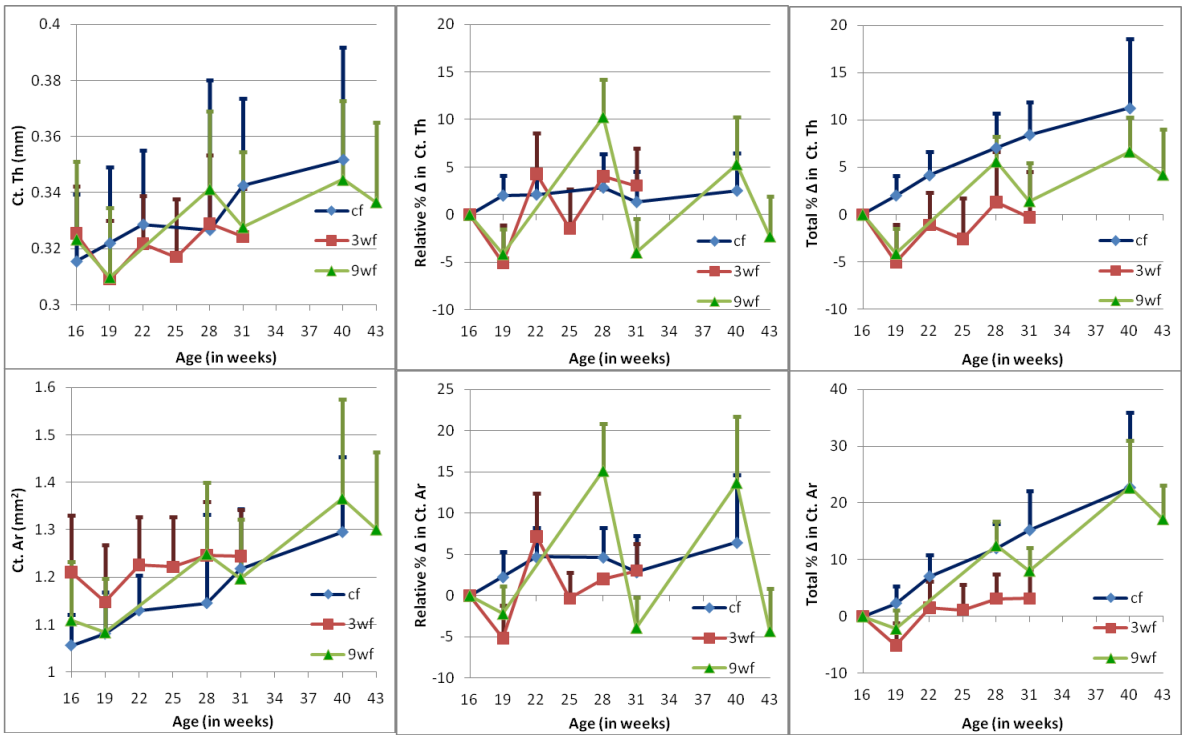

Figure 12(a)(I): Typifying morphological indices of the femoral mid-diaphysis: Ct. Th [mm] and Ct. Ar [mm^2] (Cortical Thickness and Area respectively) compared across the control (cf) and experimental (3wf, 9wf) groups in terms of mean values, relative percentage changes over subsequent timepoints, and total percentage change in value from baseline (16wks). All values are expressed as Mean+SD.

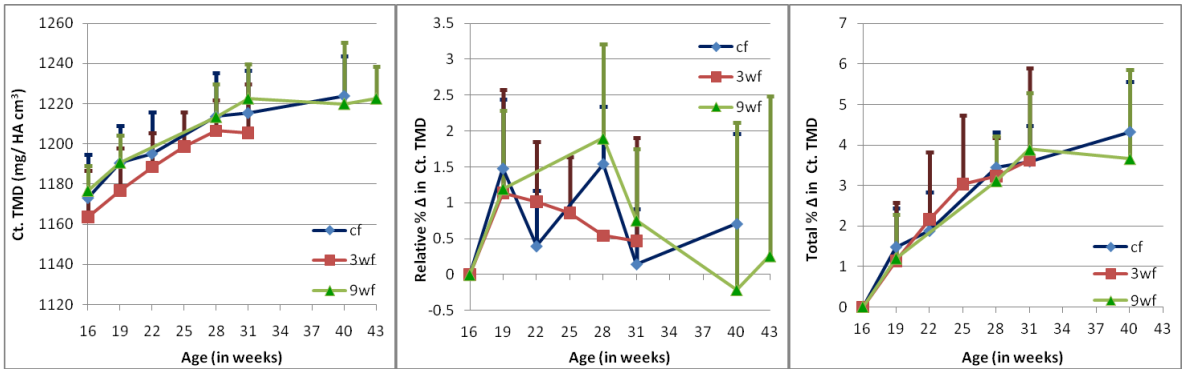

Figure 12(a)(ii): Density parameter of the femoral mid-diaphysis: Ct. TMD [mg/HA-cm^3] (Cortical Tissue Mineral Density) compared across the control (cf) and experimental (3wf, 9wf) groups in terms of mean values, relative percentage changes over subsequent timepoints, and total percentage change in value from baseline (16wks). All values are expressed as Mean+SD.

b) Surface indices

En. Ar was almost insensitive to ageing upto 5mo of age of cf, after which it increased at a slow pace of just 15% over the following 4mo. Ps. Ar, however grew linearly with time at approximately 3.5%/month. Ps. Ar of 3wf exhibited an undiagnosable trend from 22wks to 31wks. (Fig. 12(b))

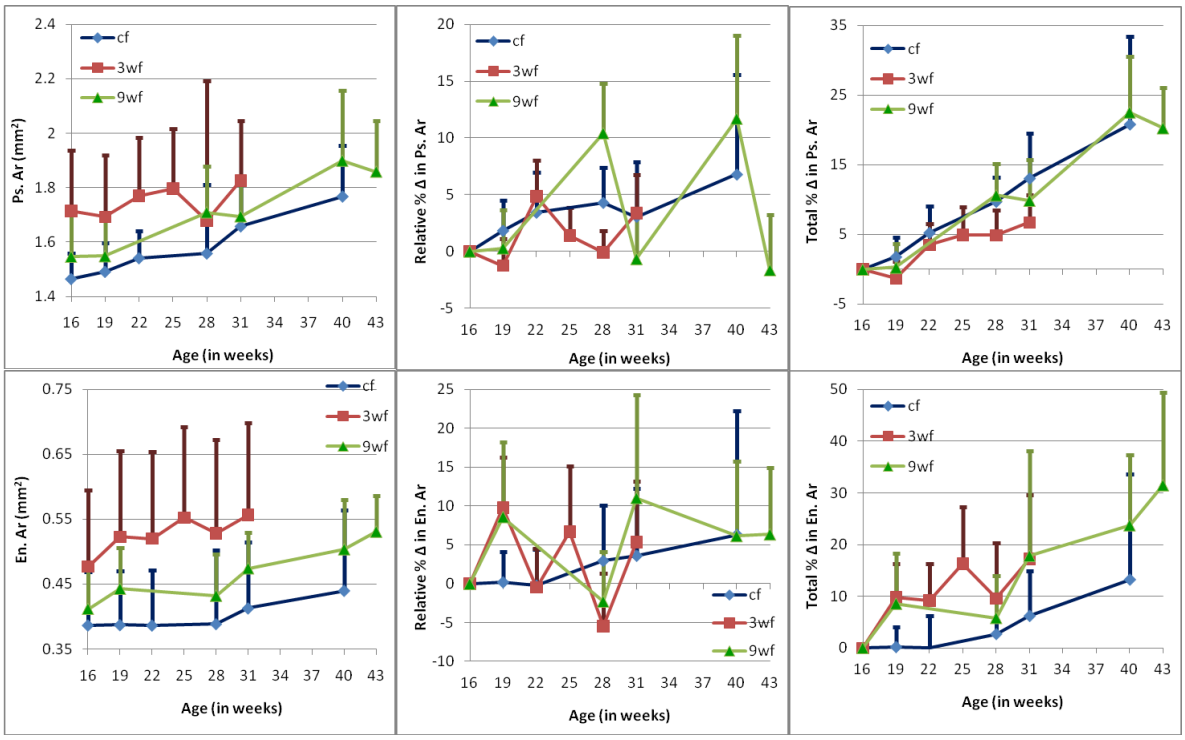

Figure 12(b): Morphological measures of the surface of the femoral mid-diaphysis: Endo. Ar and Peri. Ar, [mm^2] (Endosteal and Periosteal areas respectively) compared across the control (cf) and experimental (3wf, 9wf) groups in terms of mean values, relative percentage changes over subsequent timepoints, and total percentage change in value from baseline (16wks). All values are expressed as Mean+SD.

c) Moment of Inertia

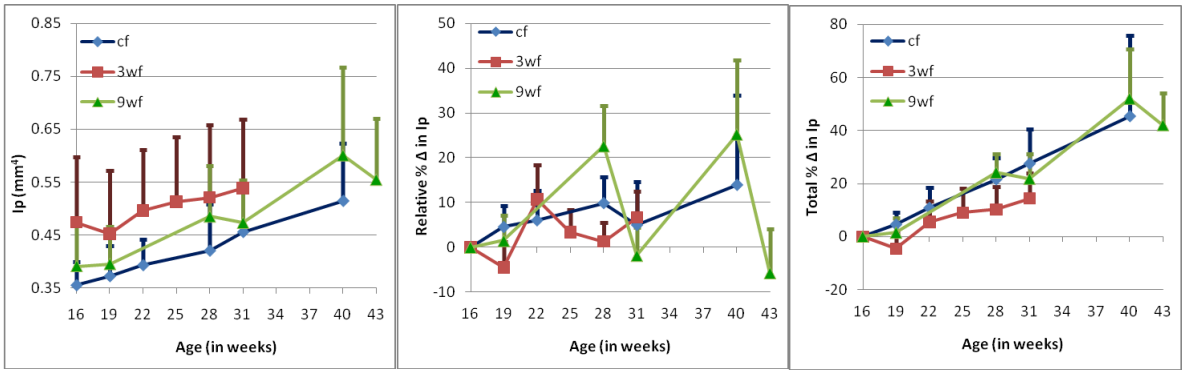

Figure 12(c): Inertial quantification of the femoral distal metaphysis: Ip[mm^4] (Principal Moment of Inertia) compared across the control (cf) and experimental (3wf, 9wf) groups in terms of mean values, relative percentage changes over subsequent timepoints, and total percentage change in value from baseline (16wks). All values are expressed as Mean+SD.

While cf's principal moment of inertia stuck to a of 7.5% per mo, 3wf experienced a 5% loss over HLU1, quickly recouped by a compensatory +15% gain from baseline, thereby a 5% recovering the 16wk-timepoint calibrated reduce in Ip after 3wks of HLU, and an additional 10% increase imitating age-

matched normally ambulating mice's Ip values. Thereafter, Ip for 3wf mice remains insensitive to HLU, though gradually meandering away from cf at 5% for every 3wks. (Fig. 12(c))

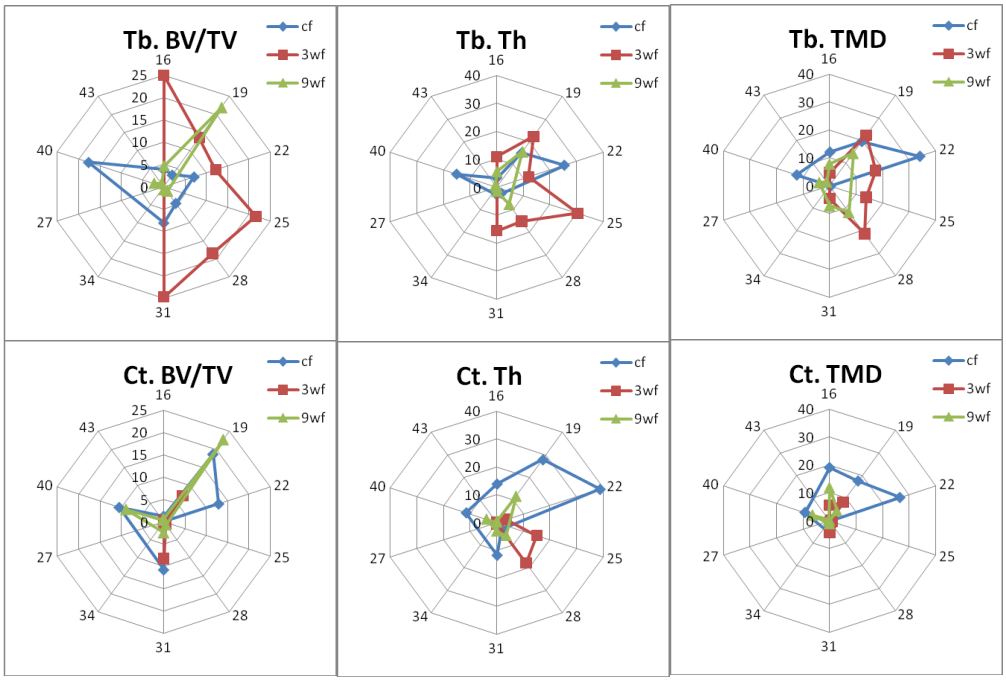

Figure 13(a): Radial plots of correlation of trabecular (Tb.) and cortical (Ct.) parameters of bone volume fraction (BV/TV), thickness (Th.), and Tissue Mineral Density (TMD) with corresponding average activity measurements for cf, 3wf, and 9wf. Correlation percentages are expressed as squares of Pearson correlation coefficients. Radial axis indicates percentages while clockwise along the web, are the timepoints in weeks.

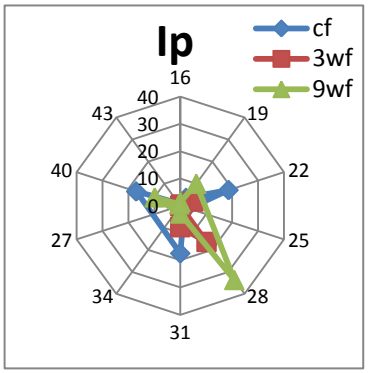

Figure 13(b): Radial plot of correlation of principal Moment of Inertia (Ip) with corresponding average activity measurements, for cf, 3wf, and 9wf. Correlation percentages are expressed as squares of Pearson correlation coefficients. Radial axis indicates percentages while clockwise along the web, are the timepoints in weeks.

4.2.3 Correlation with Activity

Correlation between trabecular indices and activity was significantly higher than the cortical for 3wf (by atleast 10%). (Fig. 13(a)) Summed across the control and experimental groups, trabecular correlation was 150% greater. Inspecting by parameter, thickness was the strongest in correlation followed by mineral density and bone volume fraction in equal intervals. Per se, activity correlated atleast 20% more strongly with the above indices post each HLU than after RA. cf and 9wf correlated much more with activity than 3wf. (Fig. 13(b) and Table 1)

Table 1. Percentage (%) of square values of Pearson correlation coefficients of morphological parameters of the femoral distal metaphysis against activity values for each animal per timepoint.

Age (in wks) ---->		16	19	22	25	28	31	34	27	40	43
Parameter	Group										
Tb. BV/TV	cf	3.85	3.25	7.16		4.59	8.12			17.73	
	3wf	24.93	13.54	12.23	21.62	18.53	24.72				
	9wf	4.62	21.85			1.30	0.75			2.29	0.88
Tb. Th	cf	3.31	15.11	25.51		2.79	2.74			15.10	
	3wf	10.88	22.37	12.01	30.34	15.02	15.55				
	9wf	5.59	15.77			7.58	1.44			0.03	0.92
Tb. TMD	cf	11.96	19.43	33.89		0.21	0.02			12.48	
	3wf	4.64	22.36	17.30	13.71	21.27	4.65				
	9wf	7.83	14.43			11.77	7.20			3.91	1.74
Ct. BV/TV	cf	1.21	18.71	12.92		0.00	10.80			10.42	
	3wf	0.18	7.13	0.17	0.01	0.70	8.27				
	9wf	0.65	22.67			0.86	2.53			8.83	0.39
Ct. Th	cf	13.92	27.96	38.77		2.92	11.71			11.58	
	3wf	0.24	0.18	3.58	15.05	17.92	0.52				
	9wf	0.56	11.80			5.76	3.06			3.96	0.17
Ct. TMD	cf	18.91	17.43	26.53		0.17	4.60			9.21	
	3wf	5.48	8.09	0.51	0.93	0.50	4.31				
	9wf	11.95	4.44			0.01	1.17			6.47	0.38
Ip	cf	0.67	3.57	18.64		2.28	17.48			17.01	
	3wf	0.01	0.47	4.99	0.00	16.38	7.83				
	9wf	1.33	9.94			33.69	2.87			9.88	0.64

4.3 MECHANICS

4.3.1 Von-Mises Stress of the Femoral Distal Metaphysis

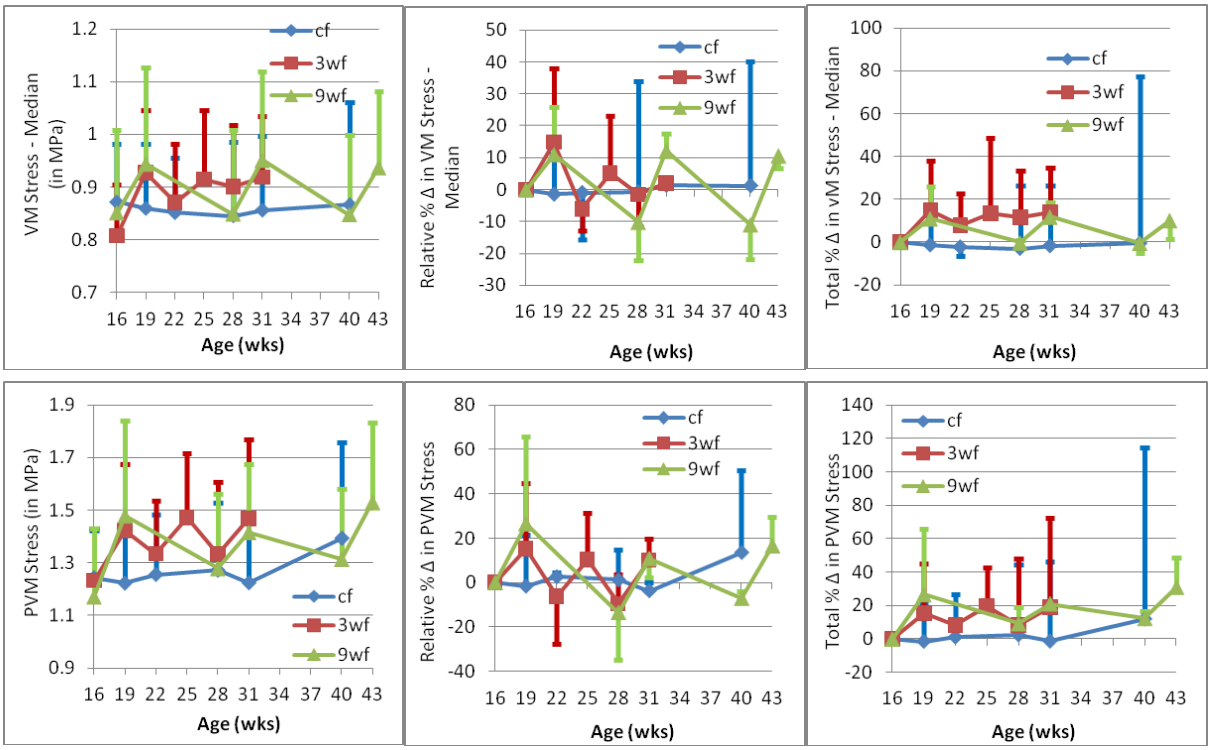

Figure 14. Mechanical stresses experienced the femoral distal metaphysis: median VM stress and PVM [MPa] (VM – Von-Mises stress) compared across the control (cf) and experimental (3wf, 9wf) groups in terms of mean values, relative percentage changes over subsequent timepoints, and total percentage change in value from baseline (16wks). All values are expressed as Mean+SD.

While 3wks RA was sufficient to only reduce stress levels by 50% of the increase over 3wks of HLU shifting 3wf away from cf at a 50% increment after each successive RA, 9wks RA reduced stresses by 200% because of which 9wf stress values meet cf post-RA.PVM increased gradually with age upto 10% in 6mo for cf. (Fig. 14)

4.3.2 Component Specificity

Tb. PVM was lower than Ct. PVM by atleast 10% (Fig. 15(a)). At baseline (16 wks), Ct. PVM (1.2MPa) was higher than Tb. PVM (1.0MPa) for all groups. Thereon, this 0.2MPa disparity progressed to 0.6MPa for 3wf at 31wks, 0.4MPa for cf at 40wks, and 9wf at 43wks. Ct. PVM also was, on average, 10% more sensitive to the experiment. Further, Tb. PVM for the 3wf group exhibited a slow time dependent increase through 28wks followed by a steep drop back to stresses around that experienced at baseline. (Fig. 15(b))

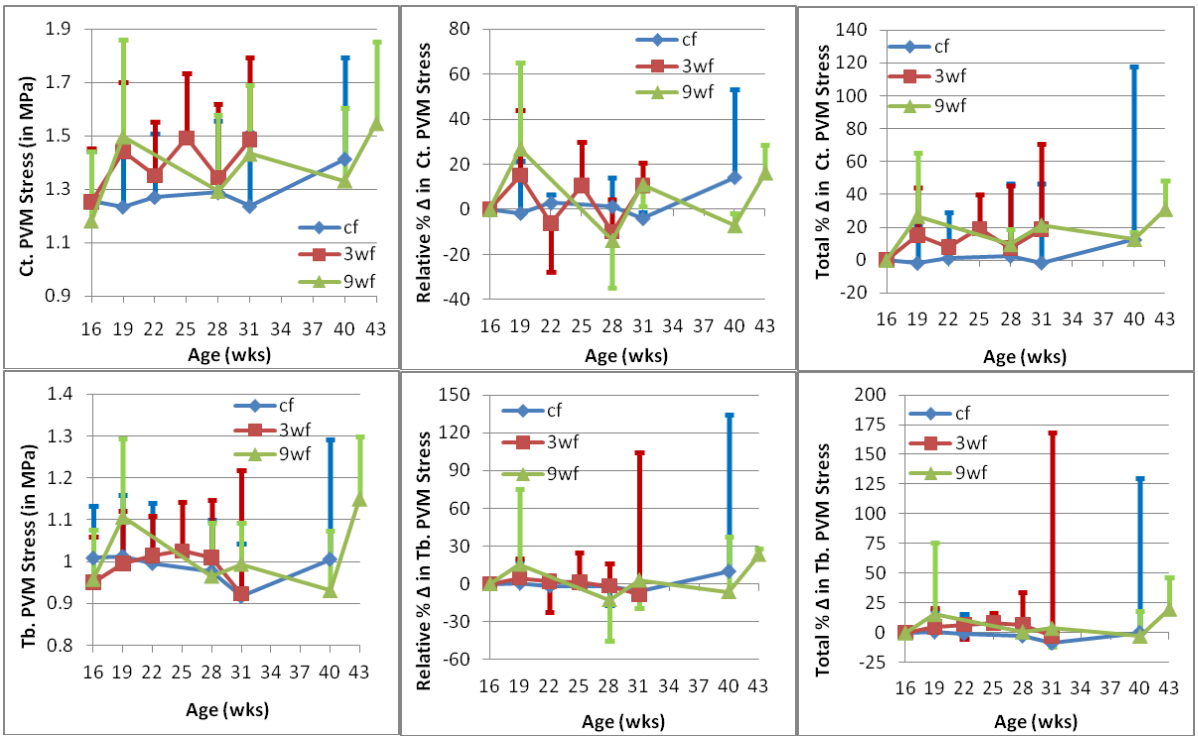

Figure 15(a): Mechanical stresses experienced the femoral distal metaphysis: Tb. PVM and Ct. [MPa] (Trabecular and Cortical Peak Von-Mises stress respectively) compared across the control (cf) and experimental (3wf, 9wf) groups in terms of mean values, relative percentage changes over subsequent timepoints, and total percentage change in value from baseline (16wks). All values are expressed as Mean+SD.

Table 2. Percentage (%) of square values of Pearson correlation coefficients of PVM stress mechanical parameter of the femoral distal metaphysis against activity values for each animal per timepoint.

Age (in wks) ---->		16	19	22	25	28	31	34	27	40	43
Parameter	Group										
PVM	cf	2.20	4.41	47.66		0.01	4.95			11.48	
	3wf	21.52	1.41	6.06	20.89	9.82	15.79				
	9wf	0.48	36.57			8.44	8.31			1.70	0.82
Ct. PVM	cf	2.19	4.65	47.63		0.01	4.45			11.36	
	3wf	20.93	1.28	5.44	20.91	9.17	13.05				
	9wf	0.44	36.66			8.78	8.04			1.54	0.85
Tb. PVM	cf	0.53	1.57	45.31		0.05	27.66			0.71	
	3wf	16.70	47.30	11.96	0.01	0.49	23.06				
	9wf	1.33	14.40			4.78	9.66			8.47	22.05

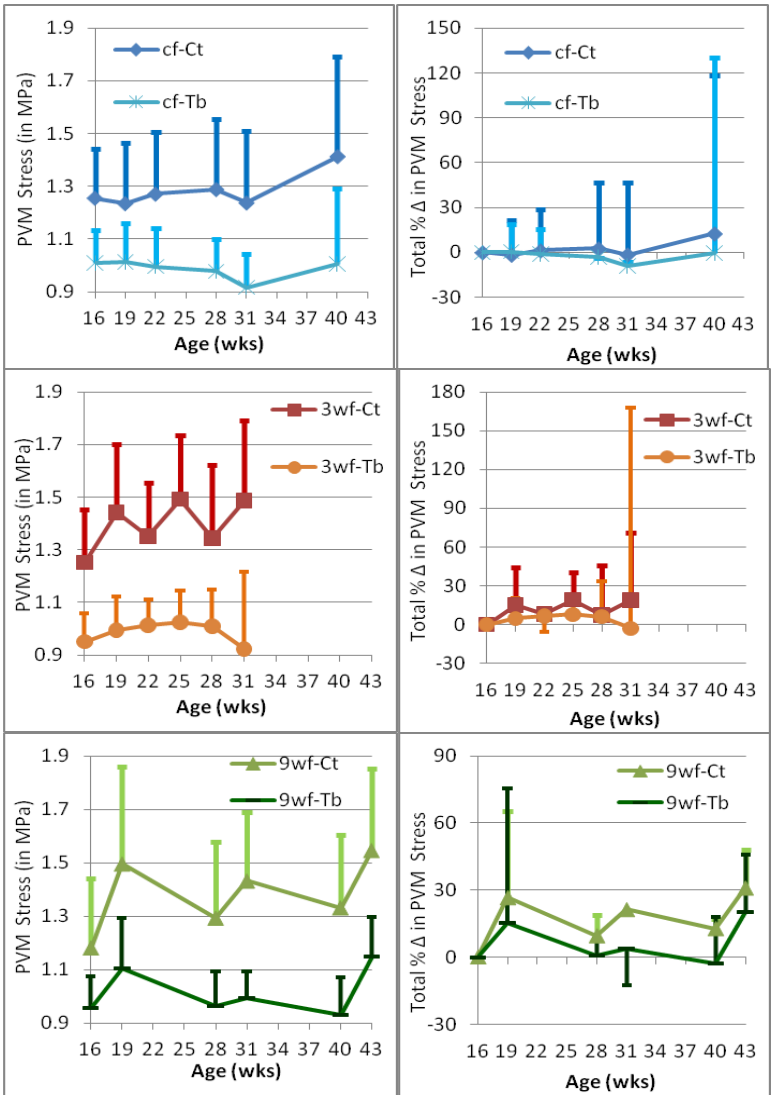

Figure 15(b): Mechanical stresses experienced the femoral distal metaphysis: PVM [MPa] (Peak Von-Mises stress respectively) compared across the control (cf) and experimental (3wf, 9wf) groups to contrast trabecular and cortical behavior in terms of mean values, and total percentage change in value from baseline (16wks). All values are expressed as Mean+SD.

4.3.3 Correlation with Activity

Strength of correlation was as high as 50% at 19wks, with Tb. PVM being greater than PVM on the net structure, and Ct. PVM at 31wks. Otherwise, PVM and Ct. PVM were very similar in percentage correlation across the 3 groups, with a 20% higher correlation for Tb. PVM. (Fig. 16, Table 2)

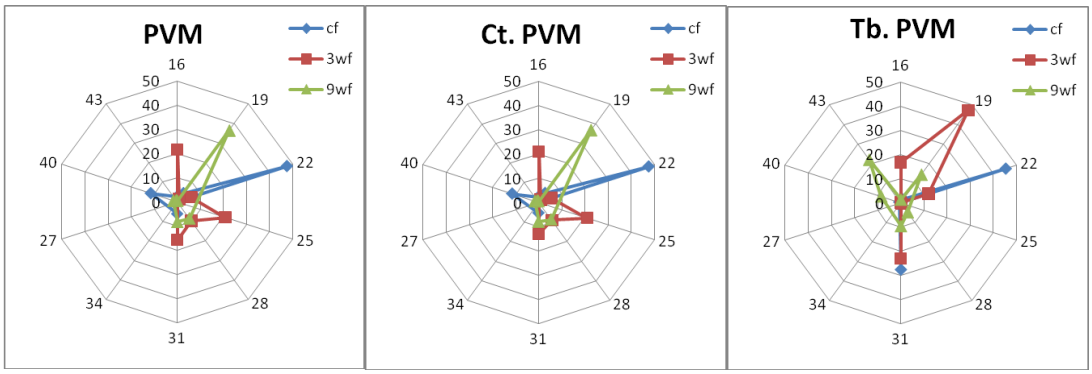

Figure 16. Radial plot of correlation of PVM of the femoral metaphysis as the net structure (PVM), cortical component alone (Ct. PVM), and trabecular compartment alone (Tb. PVM), with corresponding average activity measurements, for cf, 3wf, and 9wf. Correlation percentages are expressed as squares of Pearson correlation coefficients. Radial axis indicates percentages while clockwise along the web, are the timepoints in weeks.

4.3.4 Stress Contours with Ageing

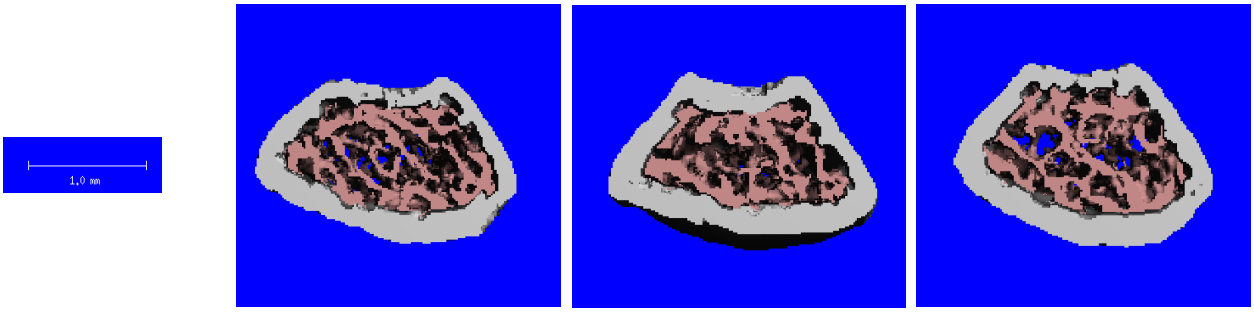

Figure 17(a)(i): Segmented files of the cross-section of the femoral distal metaphysis of the left leg of cf, 3wf, and 9wf (from left to right) at baseline (16wks) where areas shaded grey are part of the cortex while the pink spongy component is the trabeculae. Diagram is at the 1.0mm shown to the extreme left.

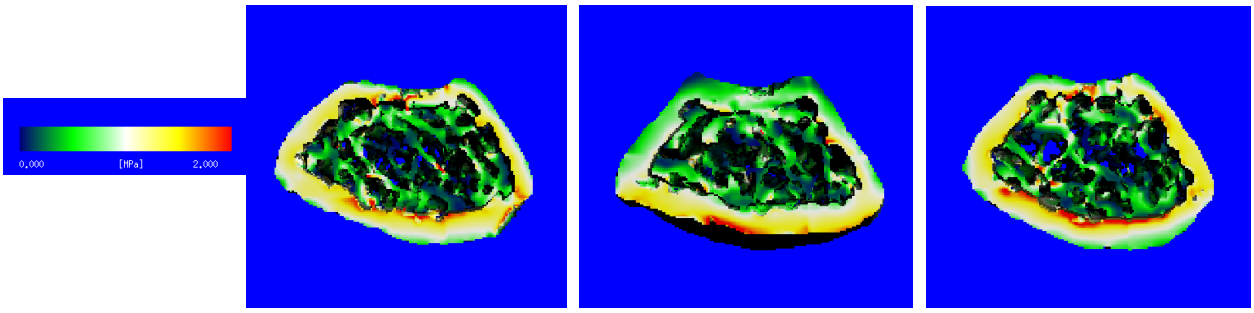

Figure 17(a)(ii): Color-contoured images of the Peak Von-Mises stresses (PVM) experienced by the the femoral distal metaphysis of the left leg of cf, 3wf, and 9wf (from left to right) at baseline (16wks) where dark green to red represents increasing PVM from 0 to 2MPa. Scale is as provided in the extreme left.

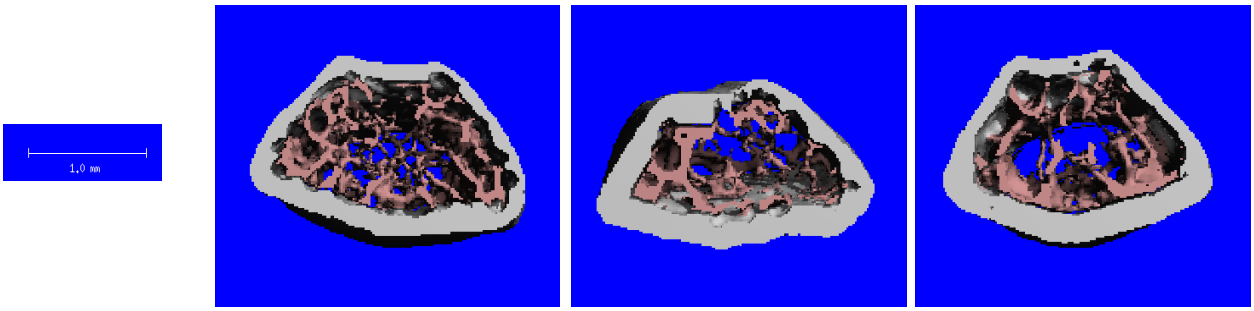

Figure 17(b)(i): Segmented files of the cross-section of the femoral distal metaphysis of the left leg of cf, 3wf, and 9wf (from left to right) at last time points of observation (40wks, 31wks, and 43wks respectively) where areas shaded grey are part of the cortex while the pink spongy component is the trabeculae. Diagram is at the 1.0mm shown to the extreme left.

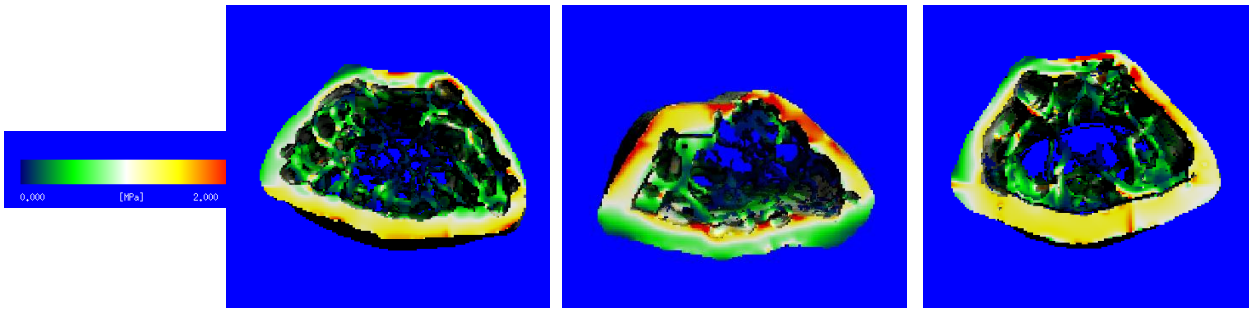

Figure 17(b)(ii): Color-contoured images of the Peak Von-Mises stresses (PVM) experienced by the the femoral distal metaphysis of the left leg of cf, 3wf, and 9wf (from left to right) at at last time points of observation (40wks, 31wks, and 43wks respectively) where dark green to red represents increasing PVM from 0 to 2MPa. 31wks for 3wf and 43wks for 9wf denote completion of experimental procedure. Scale is as provided in the extreme left.

5. DISCUSSION

Recapping the motives behind this disuse study, a central hypothesis dictated that the duration of reambulation between successive exposures to disuse was key in modulating recovery in bone quantity and quality. Specifically, hypotheses was made that individual variability in animal activity becomes inconsequential when comparing populations subjected to different loading environments, that prolonged recovery periods between multiple exposures to disuse enhances recovery of bone strength and reduces decline in musculoskeletal properties, and that the effects of disuse on the musculoskeletal properties of an animal reflect uniformly on its activity levels.

After studying the effects of disuse on a hindlimb-suspension rodent model, it was arrived at that femoral morphology, mechanics, and activity respond coherently and in a time-dependent manner, recovering significantly, the damage meted out by disuse over a reambulation period, three times as long as the duration of disuse. Activity varied only absolutely over the experiment, and differed insignifigantly within each group, indicating that variations induced by individual genetic makeup might be negligible over a sufficiently large, genetically diverse population.

activity is key to unraveling unique behavior caused by individual genetic makeup over populations exposed to the same physiological and environmental conditions of loading and unloading

activity predicts morphological and mechanical bone behavior on multiple exposures to disuse

5.1 HYPOTHESIS 1 – ACTIVITY

5.1.1 *Animal Activity does not Reveal Considerable Individual Genetic Effects for a Population experiencing the Same Loading Environment*

Animal activity indicates that each animal, despite living the same lifestyle as others within its group, behaves in a characteristic individualistic pattern. It is easy to see distinction among the magnitudes of activity in response to age, ambulation, HLU, and RA, that helps clearly delineate the high versus low responders, which is the influence of highly subjective genetic make-up. The more active animals were also the ones most sensitive to HLU and RA. Nevertheless, it is safe to say that within each litter, though the magnitudes of response among animals may have been starkly different, the pattern of age-related response remains uniform. Activity patterns are fairly reproducible across different litters, implying that though variations in activity are induced perhaps owing to individual genetic make-up of the mice, across litters, physiology is fairly comparable. This throws light on the important possibility of a reduced variability in terms of animal activity when a sufficiently large diverse population set is taken.

Activity decreased after unloading and increased after a phase of normal loading, though only mildly sensitive. However, it is clear that the rate of change in activity between subsequent time points increases with age, while the net change from baseline is fairly comparable through the experiment. Change in activity after the first exposure to disuse was often greatest in magnitude, and decided the nature of response over the following exposures to disuse as well. Activity never decreased after a period of RA, and depended only on the period of RA, not age.

5.1.2 *Activity is Independent of Nature of Exposure to Disuse*

It is interesting to note that the experimental groups (3wf and 9wf) were similar in their activity levels and trends On the other hand, the control differs, significantly and equally, from both experimental groups through 31wks, upon which 3wf completes its 3 HLUs and 2 RAs. From 31wks to 43wks, 9wf behavior mimics that of cf, enforcing normalization of activity levels upon acclimatization to repeated diuse provided a sufficient intermittent recovery time exists.

5.1.3 *Variability in Activity Between Animals Becomes Inconsequential when Comparing Populations Subjected to Different Loading Environments*

Connecting the previous two inferences, though stark outliers in animal activity exist when examining populations exposed to the same load-bearing conditions, these become insignificant when comparing populations exposed to different load-bearing environments. Outliers are few in number and span both ends of the spectrum of possible responses when a sufficiently large data set is taken. Hence, they do not skew the mean activity of the population in such a way as to weight the population's activity in any direction.

5.1.4 *Limitations*

It is hard to comment on the nature of changes, owing to this unpredictability in activity levels over loading and unloading cycles. However, it must be noted while making all these observations (activity measurements), that the standard deviations are as high as the average activity values itself. Hence, the effects of such high variance on the nature of these speculations needs to be taken into account.

Also, the unfortunate absence of data at a few timepoints for certain litters leaves only uncertain speculation about a possible unaccounted deviation in activity behaviour. However, this needs to only remain a benefit of doubt because of the insignificant minority of such points and the reproducibility of activity observed across all other litters throughout the experiment. Deviations, if any, were generally of a negligible magnitude. The effects of significant deviations were waived when averaged across the group, producing reasonable mean values.

While the third litter from the 9wf group exhibited strange behaviour in comparison to the experimental group mean, this can be discounted by the fact that this litter is comprised of only 2 animals that could possibly both be high responders.

5.2 HYPOTHESIS 2 – MORPHOLOGY AND MECHANICS

5.2.1 *Abdominal Fat and Lumbar Spine Experience Progressively Less Decay over Multiple Exposures to Disuse of Same Duration, Interspersed with Reambulation Phases that Ensured Recovery in a Duration-Dependent Manner.*

Abdominal fat morphology exhibited a consisand tent reduction over HLU and reversal over RA, with the greatest loss over the HLU1 unrecoverable over the RA1 by 3wf, but recoverable for 9wf. Beyond this first cycle of HLU and RA, animals perhaps acclimatized to disuse better and adapted thereon, thereby losing lesser adipose tissue over HLU2, fairly recoverable over RA2 even by the 3wf group, progressing to lose even less over HLU3, but insignificantly so from HLU2. TAT, SAT, and VAT were strongly correlated in their response. Lumbar spine volume projected by apparent volumetric mineral density (aVMD) echoes the same trends.

5.2.2 *Femoral Distal Metaphyseal Micro-architecture Experiences Progressively Less Decay over Multiple Exposures to Disuse of Same Duration, Interspersed with Reambulation Phases that Ensured Recovery in a Duration-Dependent Manner.*

Simulated weightlessness inducing a decrease in mineralized tissue in growing rats has been proved beyond question.[133] This study of multiple experiences of simulated weightlessness on adult mice reaffirms this. Nearly all the micro-architectural properties of the trabeculae and cortex, volumetric indices, and moments of inertia, reinforced the afore-mentioned behavior observed with abdominal fat. A golden ratio of 3 between the duration of intermittent RA between successive HLU, was sufficient to counter destructive effects to morphology encountered over the immediately prior HLU period. Contradictory to the variations in abdominal fat, 3wf (that has a ratio of 1 between the duration of intermittent RA between successive HLU) could almost never recover the damage inflicted by disuse. But upto double the degradation observed with BV/TV over HLU was regained by 9wf that has a 3X ratio between RA and HLU. This might be an important step forward to answer repeated observations made, even in the context of restoring bone calcium - the time required to restore bone calcium in growing rats exposed to disuse exceeding the time required to produce the original calcium deficit.[53]

It was also observed that endosteal measures degraded anywhere between twice and thrice as much as that of the periosteum. Trabecular thickness, interestingly, increased when bones were subjected to disuse, and was insensitive to the duration of RA. But this was justifiable by an ageing-induced slowing in growth of thickness in the age-matched controls. Similarly, tissue mineral densities for both experimental groups portrayed a very small increase over HLU1, reverting back to trends followed by other indices, but changing at a consistently increasing rate over progress through the experiment.

5.2.3 ***The Trabeculum is Most Significantly Responsible for Morphological Sensitivity of the Femoral Distal Metaphysis to Disuse. The Cortex is Fairly Insensitive to Disuse in Comparison with the Exception of Thickness, Area, and Mineral Density.***

On comparing the roles played by the bone components, the cortex might be considered insensitive to the weight-bearing functionalities of bone. Ct. BV/TV is atleast a fifteenth of Tb. BV/TV. Consistently, apparent mineral density loss experienced by the cortex is a tenth of trabecular loss.

On the other hand, both trabecular and cortical compartments experienced TMD variation within ±2% through the experiment for controls and experimental groups. Cortical thickness and area were comparable in its behavior, ranging between 50% and 75% as sensitive as their respective trabecular counterparts.

Various studies have backed this concept of significant trabecular response over the cortical[22, 24], though speculations are rife on the possible mechanisms involved. A reduced mass of mineralized tissue and accumulation of marrow fat occurred in the proximal tibia and humeral metaphyses of growing rats subjected to spaceflight. Although the bone cell population was not dramatically altered by weightlessness, osteoblast numbers in the proximal humerus declined immediately adjacent to the growth cartilage. This finding, in combination with depressed osteoblastic activity in the metaphyses, suggests that trabecular bone formation may have been inhibited during spaceflight. Also, with the exception of trabecular bone mass, the observed skeletal changes returned to normal during a 29-day postflight period.[19]

Another explanation for the decreased trabecular bone volume is the growth plate's functionality in providing calcified cartilage as a substrate for bone formation, being temporarily slowed or arrested by weightlessness,[24, 31] in turn probably due to a slowing of longitudinal bone growth. This inhibition of bone elongation in rats subjected to spaceflight and simulated weightlessness has been reported.

5.2.4 ***Femoral Mid-Diaphysis Micro-architecture is More Resilient to the Detrimental Effects of Disuse, in Comparison with the Femoral Distal Metaphysis.***

The femoral mid-diaphysis mimicked abdominal fat, lumbar spine, and femoral distal metaphyseal response to the experimental design, experiencing recovery of disuse inflicted damage in a time-dependent manner with RA and reasserting that 3X RA/HLU ratio for optimal recovery. However, consequent exposures to disuse did not mellow down the detrimental effects on the diaphysis (as against the metaphysis) for both experimental groups, ruling out the possibility of acclimatization or adaptation to repeated exposures to disuse. But indicators pointed towards the fact that, perhaps, the diaphysis was more resilient to disuse-induced deterioration because the rate of recovery experienced in even a 3wk RA period (3wf) was significantly higher than corresponding metaphyseal response. Cortical thickness, area, mineral density and moment of inertia pointed in this localized site-specific response, TMD experiencing sheer age-related natural decay after about 28wks of age.

Surface parameters behave in an interesting fashion at the diaphysis. Endosteal area in normally loaded animals itself is rather stable with time. In tune with this nature, the experimental groups increase in area on disuse and reverted to age-matched controls upon RA, but faithful to the 3X RA/HLU ratio. On the other hand, the periosteal equivalent is predictable with reduction on disuse and vice-versa upto 43wks for 9wf, but only till 22wks in case of the 3wf mice. Relative changes over subsequent intervals of experimental protocol across the 9wf and 3wf group proved insensitive to the numbers of exposures to HLU, time period of disuse and intermittent RA. This may have occurred because of the lack of trabecular content in this region. This is important because spaceflight is known to result in a prominent skeletal defect at the periosteal surface of the tibia diaphysis to growing rats. This defect separated the bone formed in space from that formed following spaceflight. The altered bone was inferior to normal bone in resistance to abrasion and may be partially responsible for the decrease in torsional strength observed after spaceflight.[134]

5.2.5 ***Femoral Distal Metaphysis Experiences is Subjected to Progressively Increasing Stress Levels over Multiple Exposures to Disuse of Same Duration, Interspersed with Reambulation Phases that Ensured Recovery in a Duration-Dependent Manner.***

As anticipated, stress levels peak on unloading and relax after loading cycles. Clearly, 9wf stresses return to normal ambulatory levels after the experiment, while 3wf experiences much higher residual stresses. Bone mechanics reaffirms the results produced by morphology. Trabeculae also adapted to disuse with time, as is reflected by 3wf over its third unloading cycle (28wks to 31wks) over which it closely resembled control group stresses.

While the Peak Von-Mises stress attained reduces over consecutive HLUs, the medial VM stress values themselves are fairly invariant, owing to the extremely high ratio of nodes experiencing peak stresses as against the total number of nodes in the metaphyseal section. Therefore, it is important to keep in mind that though 3wf is insufficient to temper the increasing in median VM stress values caused by an equal period of HLU, PVM stress can be brought back to that of age-matched controls over the same duration.

5.2.6 *The Cortex is Most Significantly Responsible for Mechanical Sensitivity of the Femoral Distal Metaphysis to Disuse. The Trabeculum is Fairly Insensitive in Comparison.*

The contrasting aspect between femoral metaphyseal mechanics and morphology was the consistent increased sensitivity of the cortex, owing to its structural and functionality under load-bearing. Being the hard outer shell, it shielded the spongy trabeculae enclosed within, which is consequently far less invariant in its mechanical response to disuse. The less stiff trabecular bone is relatively rubbery and can withstand higher strain magnitudes. It experiences failure when deformed to 7% of its original length while the cortex can only last uptil 2% as proclaimed by other studies.[135]

5.2.7 *Prolonging recovery periods between multiple exposures to disuse enhances recovery of bone strength and reduces decline in musculoskeletal properties*

Based on the previous inferences, the second hypothesis proved to be true – that prolonging recovery periods between multiple exposures to disuse enhanced the recovery in bone deterioration experienced during disuse. An interesting contradictory observation might be made that the desensitization that multiple exposures to disuse causes the 3wk RA group to recover more bone than the 9wk RA group at 31wks. Over this period, while the former has completed all 3 exposures to disuse and the 2 intermittent exposures to RA, over which period the latter undergoes 2 HLU durations and 1 intermittent RA. This might paint the picture that the 3wk RA period is more optimal because after this 31wk point, it does not experience any further disuse. Hence, it can only increasingly recover bone. However, an important factor to take into account is what all previous studies have shown, that recovery after disuse is never complete, only partial.[24, 34, 54, 55] Since this study does not include long-term observations in bone parameters that conclusively prove complete recovery in the 3wk-RA or 3wf group, it is important to understand that the 9wk-RA group, despite experiencing greater loss over each exposure to disuse and a longer overall experiment duration, does prove a definitive recovery at 43wks. Keeping in mind this limitation and assumption, prolonging the recovery period does conclusively enhance recovery in musculoskeletal and mechanical characteristics of bone.

5.2.8 *Limitations*

Though the microCT cannot be ignored in its capacity to qualify and quantify bone, and evaluation of orthogonal mechanical properties of bone have been well tested and documented, [125, 136] such analysis is incomplete without more definitive and conclusive measures such as Histomorphometry that are indispensable for providing a complete picture of the changes experienced by bone. Likewise, though the finite element analysis is most competent in simulating mechanical tests, it cannot compete with *in vitro* equivalents such as the 3-point bending test or nanoindentation. FEA, and microCT imaging is additionally limited by practical factors such resolution, force and displacement tolerances.

5.3 HYPOTHESIS 3 – CORRELATING ACTIVITY WITH FEMORAL MORPHOLOGY AND MECHANICS

5.3.1 ***The Effects of Disuse on Musculoskeletal Properties of an Animal Reflect Uniformly on Its Activity.***

Clearly, activity did not establish a strong correlation with morphological and mechanical variations induced by disuse (all within 50%). However, it may be meaningful to map the trends of correlation through the 6mo experimental period. Interpretations were made on a parametric, experimental phase (i.e., HLU or RA), component- and group-wise basis.

Correlations could not be associated with any specific quantification of micro-architecture. However, greater correlations were observed post-suspensions rather than after phases of normal loading. Clearly, the pivotal role of trabeculae was reinforced by the strength of its correlations being more 150% as that of the cortex – even for the PVM stresses that the cortex was much more sensitive to. Interestingly, control group correlated most with activity closely matched by 9wf, perhaps an indication of sufficient recovery time for return to normal movement – a clear indication of better recovery of bone micro-architecture – as against the 3wf group that was significantly lower in its correlation.

On an independent note, activity, and morphology are synchronous in their most significant response to disuse occurring over the very first exposure to disuse. Nevertheless, relating bone structure, activity, and mechanical integrity, the reason behind non-uniformity in the way animals with low bone mass responded, correlates with prognosis for humans. This has been confirmed by cellular studies that reason that while some bone cells are constantly undergoing breakdown and repair, others are in a normal state of homeostasis. The former will, therefore, experience reduced mechanical properties since its resorption cavities might act as stress risers, triggering crack propagation in the lag time between breakdown and repair.[137, 138] This can be confirmed in conjunction with a similar animal suspension study that declared that femur composition, cross-sectional geometry, and strength were

significantly altered by disuse after 2 weeks, but not after 1 week. Femur mineralization was affected by time, but not by suspension, and bending yield stress was affected by suspension but not by time.[139]

5.4 LIMITATIONS

Though there is a wealth of evidence in support of the harmful effects of spaceflight on the skeleton, that these effects are progressive, [140, 141] and that non-weight bearing bones are less affected than the weight-bearing ones, [142-145] certain limitations plague these kind of studies. However, sufficient emphasis needs to be placed on the fact that skeletal abnormalities have not been observed in all disuse studies, and changes have not always been detected (in weight-bearing bones).[146-150] Contrasts to these usual observations has been reported in adult humans wherein renormalization of bone lost during bed rest occurred as rapidly or more rapidly than the original bone was lost.[151, 152] These negative studies suggest that the effects of spaceflight may be influenced by caging conditions, age, or other unknown factors.

The study is also limited in its capacity for analysis, owing to the lack of a common endpoint that permits statistical comparison for significant differences concomitantly with age and time. Also, the long-term effects of such a procedure of disuse remain to be explored. Also, the rat is an established model for many aspects of human bone metabolism, but it has some limitations. The lack of a well-developed Haversion system renders most small mammals, including the rat, unsuitable for investigating the effects of spaceflight on cortical bone remodeling.[59]

5.5 IMPLICATIONS

Although the mechanisms are not likely to be the same in aging and space flight, there are common elements. For example, strategies developed to prevent disuse bone loss or to enhance the rate of recovery following space flight might have direct applicability to clinical medicine. The development of strategies to encourage or enhance bone formation following space flight may be as important as implementing countermeasures during flight.[34]

5.6 SUMMARY

In summary, femoral behavior was studied in response to 3 exposures to 3wks of unloading each, 1 experimental group receiving intermittent reambulation of 3wks duration (3wf) and another of 9wks reambulation (9wf). Over this experimental period, it was inferred that while activity patterns did not

offer significant information on the role played by individual genetic constitution in unique behavior to similar environmental, physical, and physiological lifestyles, it offered hope that the role of genetics could be insignificant over a sufficiently large genetically diverse population. At the same time, activity levels were affected considerably by disuse itself, but not by variations in the patterns of exposure to disuse. Abdominal fat and femoral micro-architecture was sensitive to unloading in terms of its morphology and mechanics, experiencing greater deterioration over successive exposures to disuse that could be overcome at a percentage in proportion with the unloading and reambulation duration ratios. While equal durations of unloading and reambulation durations was sufficient to recover loss in fat faced due to disuse, a reambulation period 3 times as long as a constant disuse duration was generally sufficient to optimally recover bone loss of the femoral sites. The femoral mid-diaphysis exhibited relative site-specific resilience to disuse in comparison with the distal metaphysis. Likewise, in both sites, the cortex exhibited significant resilience in contrast with the trabecular compartment. Mechanical stresses experienced by the femoral metaphysis was significantly increased post disuse, with the corresponding trends mimicking morphological behavior. However, the cortex was more sensitive than the trabeculae in terms of stress and load-bearing. When activity was correlated with morphology and mechanics, no clear prediction was achieved. But if confirmed previous inferences.

In totality, bone architecture experienced continued degradation on multiple exposures to disuse, recovered in degrees based on the duration of reambulation between successive unloading periods.

REFERENCES

1. Marks, S.C. and S.N. Popoff, *Bone Cell Biology - the Regulation of Development, Structure, and Function in the Skeleton.* American Journal of Anatomy, 1988. **183**(1): p. 1-44.
2. Wolff, J., *Das gesetz der transformation der knochen.* 1892.
3. Turner, C.H., A. Chandran, and R.M. Pidaparti, *The anisotropy of osteonal bone and its ultrastructural implications.* Bone, 1995. **17**(1): p. 85-9.
4. Hayes, W.C., *Bone Mechanics.* Annals of Biomedical Engineering, 1983. **11**(1): p. 37-38.
5. Ranalli, D.N., D.M. Lancaster, and A.L. Mullig, *Lip service.* N Y State Dent J, 1995. **61**(7): p. 34-8.
6. Riggs, B.L. and L.J. Melton, 3rd, *Osteoporosis and age-related fracture syndromes.* Ciba Foundation Symposium, 1988. **134**: p. 129-42.
7. Hert, J., P. Fiala, and M. Petrtyl, *Osteon orientation of the diaphysis of the long bones in man.* Bone, 1994. **15**(3): p. 269-277.
8. Burstein, A.H., D.T. Reilly, and M. Martens, *Aging of bone tissue: mechanical properties.* Journal of Bone & Joint Surgery - American Volume, 1976. **58**(1): p. 82-6.
9. Brown, T.D. and A.B. Ferguson, Jr., *The development of a computational stress analysis of the femoral head. Mapping tensile, compressive, and shear stress for the varus and valgus positions.* Journal of Bone & Joint Surgery - American Volume, 1978. **60**(5): p. 619-29.
10. Mosekilde, L., A. Viidik, and L.E. Mosekilde, *Correlation between the compressive strength of iliac and vertebral trabecular bone in normal individuals.* Bone, 1985. **6**: p. 291-295.
11. Galante, J., W. Rostoker, and R.D. Ray, *Physical properties of trabecular bone.* Calcified tissue research, 1970. **5**(3): p. 236-46.
12. Einhorn, T.A., *Bone strength: the bottom line.* Calcif Tissue Int, 1992. **51**(5): p. 333-9.
13. Carter, D., D. Fyhrie, and R. Whalen, *Trabecular bone density and loading history: regulation of connective tissue biology by mechanical energy.* Journal of biomechanics, 1987. **20**(8): p. 785-787, 789-794.
14. Whalen, R., D. Carter, and C. Steele, *Influence of physical activity on the regulation of bone density.* Journal of biomechanics, 1988. **21**(10): p. 825-837.
15. Hughes-Fulford, M., *Altered cell function in microgravity.* Exp Gerontol, 1991. **26**(2-3): p. 247-56.
16. Garetto, L.P., et al., *Preosteoblast production in COSMOS 2044 rats: short-term recovery of osteogenic potential.* J Appl Physiol, 1992. **73**(2 Suppl): p. 14S-18S.
17. Young, D., W. Niklowitz, and C. Steele, *Tibial changes in experimental disuse osteoporosis in the monkey.* Calcified Tissue International, 1983. **35**(1): p. 304-308.
18. Minaire, P., et al., *Quantitative histological data on disuse osteoporosis.* Calcified Tissue International, 1974. **17**(1): p. 57-73.
19. Jee, W.S., et al., *Effects of spaceflight on trabecular bone in rats.* The American journal of physiology, 1983. **244**(3): p. R310-4.
20. Vico, L., et al., *Effects of weightlessness on phospho-calcium metabolism and its hormonal regulation in man during the 51 G Franco-American space flight.* Pathologie-biologie, 1988. **36**(2): p. 144.
21. Caillot-Augusseau, A., et al., *Bone formation and resorption biological markers in cosmonauts during and after a 180-day space flight (Euromir 95).* Clinical chemistry, 1998. **44**(3): p. 578-85.
22. Collet, P., et al., *Effects of 1- and 6-month spaceflight on bone mass and biochemistry in two humans.* Bone, 1997. **20**(6): p. 547-51.
23. Heer, M., et al., *Calcium metabolism in microgravity.* European journal of medical research, 1999. **4**(9): p. 357.

24. Lang, T., et al., *Cortical and Trabecular Bone Mineral Loss From the Spine and Hip in Long Duration Spaceflight.* Journal of Bone and Mineral Research, 2004. **19**(6): p. 1006-1012.
25. Carmeliet, G., G. Nys, and R. Bouillon, *Microgravity Reduces the Differentiation of Human Osteoblastic MG 63 Cells.* Journal of Bone and Mineral Research, 1997. **12**(5): p. 786-794.
26. Kumei, Y., et al., *Microgravity induces prostaglandin E2 and interleukin-6 production in normal rat osteoblasts: role in bone demineralization.* Journal of biotechnology, 1996. **47**(2-3): p. 313-324.
27. Van Loon, J.J., et al., *Decreased mineralization and increased calcium release in isolated fetal mouse long bones under near weightlessness.* J Bone Miner Res, 1995. **10**(4): p. 550-7.
28. Burger, E. and J. Klein-Nulend, *Microgravity and bone cell mechanosensitivity.* Bone, 1998. **22**(5): p. 127S-130S.
29. Burger, E.H. and J.P. Veldhuijzen, *Influence of mechanical factors of bone formation, resorption and growth in vitro.* Bone, 1993. **7**: p. 37-56.
30. Noble, B.S. and J. Reeve, *Osteocyte function, osteocyte death and bone fracture resistance.* Molecular and cellular endocrinology, 2000. **159**(1-2): p. 7-13.
31. Vico, L., et al., *Effects of long-term microgravity exposure on cancellous and cortical weight-bearing bones of cosmonauts.* Lancet, 2000. **355**(9215): p. 1607-11.
32. Frost, H.M., *The mechanostat: a proposed pathogenic mechanism of osteoporoses and the bone mass effects of mechanical and nonmechanical agents.* Bone and mineral, 1987. **2**(2): p. 73.
33. Rubin, C.T. and L. Lanyon, *Regulation of bone formation by applied dynamic loads.* The Journal of Bone and Joint Surgery, 1984. **66**(3): p. 397.
34. LeBlanc, A. and V. Schneider, *Can the adult skeleton recover lost bone?* Experimental gerontology, 1991. **26**(2-3): p. 189-201.
35. Longnecker, D.E. and R.A. Molins, *A risk reduction strategy for human exploration of space: a review of NASA's Bioastronautics Roadmap*. 2006: Natl Academy Pr.
36. Buckey, J., et al., *Orthostatic intolerance after spaceflight.* Journal of Applied Physiology, 1996. **81**(1): p. 7.
37. Levine, B.D., et al., *Maximal exercise performance after adaptation to microgravity.* Journal of Applied Physiology, 1996. **81**(2): p. 686.
38. Watenpaugh, D.E. and A.R. Hargens, *The cardiovascular system in microgravity.* 1996.
39. Morey Holton, E.R., et al., *The skeleton and its adaptation to gravity.* 1996.
40. Michel, E.L., R.S. Johnston, and L.F. Dietlein, *Biomedical results of the Skylab Program.* Life sciences and space research, 1976. **14**: p. 3-18.
41. Young, L.R., et al., *Spatial orientation in weightlessness and readaptation to earth's gravity.* Science, 1984. **225**(4658): p. 205.
42. Smith, S.M., et al., *Bone markers, calcium metabolism, and calcium kinetics during extended-duration space flight on the mir space station.* Journal of Bone & Mineral Research, 2005. **20**(2): p. 208-18.
43. Rambaut, P.C. and R.S. Johnston, *Prolonged weightlessness and calcium loss in man.* Acta astronautica, 1979. **6**(9): p. 1113-22.
44. Smith, S.M., et al., *Collagen cross-link excretion during space flight and bed rest.* Journal of Clinical Endocrinology & Metabolism, 1998. **83**(10): p. 3584-3591.
45. Whedon, G.D., et al., *Mineral and nitrogen balance study observations: the second manned Skylab mission.* Aviation, space, and environmental medicine, 1976. **47**(4): p. 391-6.
46. Lang, T.F., et al., *Adaptation of the proximal femur to skeletal reloading after long-duration spaceflight.* Journal of bone and mineral research : the official journal of the American Society for Bone and Mineral Research, 2006. **21**(8): p. 1224-30.

47. Dupui, P., et al., *Balance and gait analysis after 30 days-6 degrees bed rest: influence of lower-body negative-pressure sessions.* Aviation, space, and environmental medicine, 1992. **63**(11): p. 1004.
48. Fortney, S.M., V.S. Schneider, and J.E. Greenleaf, *The physiology of bed rest.* 1996.
49. Leblanc, A.D., et al., *Bone mineral loss and recovery after 17 weeks of bed rest.* J Bone Miner Res, 1990. **5**(8): p. 843-50.
50. LeBlanc, A., et al., *Calcium absorption, endogenous excretion, and endocrine changes during and after long-term bed rest.* Bone, 1995. **16**(4 Suppl): p. 301S-304S.
51. Lueken, S.A., et al., *Changes in markers of bone formation and resorption in a bed rest model of weightlessness.* Journal of Bone and Mineral Research, 1993. **8**(12): p. 1433-1438.
52. Vico, L., et al., *Effects of a 120 day period of bed-rest on bone mass and bone cell activities in man: attempts at countermeasure.* Bone Miner, 1987. **2**(5): p. 383-94.
53. Sessions, N.D., et al., *Bone response to normal weight bearing after a period of skeletal unloading.* The American journal of physiology, 1989. **257**(4 Pt 1): p. E606-10.
54. LeBlanc, A., Shackelford, L., Schneider, V., *Future human bone research in space.* Bone, 1998. **22**: p. 113S-116S.
55. Sibonga, J., et al., *Recovery of spaceflight-induced bone loss: bone mineral density after long-duration missions as fitted with an exponential function.* Bone, 2007. **41**(6): p. 973-978.
56. Malakoff, D., *The rise of the mouse, biomedicine's model mammal.* Science, 2000. **288**(5464): p. 248.
57. Morey-Holton, E. and T.J. Wronski, *Animal models for simulating weightlessness.* Physiologist, 1981. **24**: p. 545-548.
58. Adams, G.R., F. Haddad, and K.M. Baldwin, *Time course of changes in markers of myogenesis in overloaded rat skeletal muscles.* Journal of Applied Physiology, 1999. **87**(5): p. 1705.
59. Turner, R.T., *Invited review: what do we know about the effects of spaceflight on bone?* J Appl Physiol, 2000. **89**(2): p. 840-7.
60. Eisman, J.A., *Genetics of osteoporosis.* Endocr Rev, 1999. **20**(6): p. 788-804.
61. Nordin, B.E., et al., *Osteoporosis and osteomalacia.* Clinics in endocrinology and metabolism, 1980. **9**(1): p. 177-205.
62. Obermayer Pietsch, B.M., et al., *Association of the vitamin D receptor genotype BB with low bone density in hyperthyroidism.* Journal of Bone and Mineral Research, 2000. **15**(10): p. 1950-1955.
63. Morrison, N.A., et al., *Prediction of bone density from vitamin D receptor alleles.* Nature, 1994. **367**(6460): p. 284-287.
64. Cooper, G.S. and D.M. Umbach, *Are vitamin D receptor polymorphisms associated with bone mineral density? A meta analysis.* Journal of Bone and Mineral Research, 1996. **11**(12): p. 1841-1849.
65. Peacock, M., *Vitamin D receptor gene alleles and osteoporosis: a contrasting view.* Journal of Bone and Mineral Research, 1995. **10**(9): p. 1294-1297.
66. Hustmyer, F., et al., *Polymorphism at an Sp1 binding site of COL1A1 and bone mineral density in premenopausal female twins and elderly fracture patients.* Osteoporosis international, 1999. **9**(4): p. 346-350.
67. Yim, C.H., et al., *Association of estrogen receptor gene microsatellite polymorphism with annual changes in bone mineral density in Korean women with hormone replacement therapy.* Journal of bone and mineral metabolism, 2005. **23**(5): p. 395-400.

68. Yamada, Y., et al., *Association of a polymorphism of the transforming growth factor-beta1 gene with genetic susceptibility to osteoporosis in postmenopausal Japanese women.* Journal of Bone & Mineral Research, 1998. **13**(10): p. 1569-76.
69. LeBlanc, A., et al., *Bone mineral and lean tissue loss after long duration space flight.* J Musculoskelet Neuronal Interact, 2000. **1**(2): p. 157-60.
70. Squire, M., et al., *Baseline bone morphometry and cellular activity modulate the degree of bone loss in the appendicular skeleton during disuse.* Bone, 2008. **42**(2): p. 341-9.
71. Judex, S., et al., *Genetically linked site-specificity of disuse osteoporosis.* J Bone Miner Res, 2004. **19**(4): p. 607-13.
72. Robling, A. and C. Turner, *Mechanotransduction in bone: genetic effects on mechanosensitivity in mice.* Bone, 2002. **31**(5): p. 562-569.
73. Robling, A.G., et al., *Evidence for a skeletal mechanosensitivity gene on mouse chromosome 4.* The FASEB Journal, 2003. **17**(2): p. 324.
74. Kodama, Y., et al., *Cortical tibial bone volume in two strains of mice: effects of sciatic neurectomy and genetic regulation of bone response to mechanical loading.* Bone, 1999. **25**(2): p. 183-190.
75. Kodama, Y., et al., *Exercise and mechanical loading increase periosteal bone formation and whole bone strength in C57BL/6J mice but not in C3H/Hej mice.* Calcified Tissue International, 2000. **66**(4): p. 298-306.
76. Koller, D., et al., *Genome screen for QTLs contributing to normal variation in bone mineral density and osteoporosis.* Journal of Clinical Endocrinology & Metabolism, 2000. **85**(9): p. 3116.
77. Kesavan, C., et al., *Identification of genetic loci that regulate bone adaptive response to mechanical loading in C57BL/6J and C3H/HeJ mice intercross.* Bone, 2006. **39**(3): p. 634-643.
78. Beamer, W., et al., *Genetic variability in adult bone density among inbred strains of mice.* Bone, 1996. **18**(5): p. 397-403.
79. Judex, S., L.R. Donahue, and C. Rubin, *Genetic predisposition to low bone mass is paralleled by an enhanced sensitivity to signals anabolic to the skeleton.* FASEB J, 2002. **16**(10): p. 1280-2.
80. Judex, S., et al., *Genetically based influences on the site-specific regulation of trabecular and cortical bone morphology.* J Bone Miner Res, 2004. **19**(4): p. 600-6.
81. Bloomfield, S.A., et al., *Site- and compartment-specific changes in bone with hindlimb unloading in mature adult rats.* Bone, 2002. **31**(1): p. 149-57.
82. Tilton, F.E., J.J. Degioanni, and V.S. Schneider, *Long-term follow-up of Skylab bone demineralization.* Aviation, space, and environmental medicine, 1980. **51**(11): p. 1209-13.
83. Smith, M., N. Aeronautics, and H. Space Administration. Lyndon B. Johnson Space Center, TX, *Bone mineral measurement: Experiment M 078*. 1977.
84. Schneider, V., et al. *Space flight bone loss and change in fat and lean body mass*.
85. Squire, M., et al., *Genetic variations that regulate bone morphology in the male mouse skeleton do not define its susceptibility to mechanical unloading.* Bone, 2004. **35**(6): p. 1353-1360.
86. McCarthy, I., et al., *Investigation of bone changes in microgravity during long and short duration space flight: comparison of techniques.* Eur J Clin Invest, 2000. **30**(12): p. 1044-54.
87. Grigoriev, A., et al., *Clinical and physiological evaluation of bone changes among astronauts after long-term space flights].* Aviakosmicheskaia i ekologicheskaia meditsina= Aerospace and environmental medicine, 1998. **32**(1): p. 21.
88. Globus, R.K., D.D. Bikle, and E. Morey-Holton, *The temporal response of bone to unloading.* Endocrinology, 1986. **118**(2): p. 733.
89. Halloran, B., et al., *The role of 1,25-dihydroxyvitamin D in the inhibition of bone formation induced by skeletal unloading.* Endocr Res, 1986(118): p. 948-954.

90. Wronski, T.J. and E.R. Morey-Holton, *Skeletal response to simulated weightlessness: a comparison of suspension techniques.* Aviation, space, and environmental medicine, 1987. **58**(1): p. 63-8.
91. Vogel, J.M., *Bone mineral measurement: Skylab experiment M-078.* Acta astronautica, 1975. **2**(1-2): p. 129-39.
92. Stupakov, G.P., et al., *[Evaluation of the changes in the bone structures of the human axial skeleton in prolonged space flight].* Kosm Biol Aviakosm Med, 1984. **18**(2): p. 33-7.
93. Oganov, V.S., et al., *The state of human bone tissue during space flight.* Acta astronautica, 1991. **23**: p. 129-33.
94. Giangregorio, L. and C.J.R. Blimkie, *Skeletal adaptations to alterations in weight-bearing activity: a comparison of models of disuse osteoporosis.* Sports Medicine, 2002. **32**(7): p. 459-476.
95. Gupta, S., et al., *Loss and recovery of musculoskeletal quantity and quality upon multiple exposures to microgravity.* 2011.
96. Cann, C.E. and R.R. Adachi, *Bone resorption and mineral excretion in rats during spaceflight.* American Journal of Physiology-Regulatory, Integrative and Comparative Physiology, 1983. **244**(3): p. R327.
97. Vico, L., et al., *Effects of weightlessness on bone mass and osteoclast number in pregnant rats after a five-day spaceflight (COSMOS 1514).* Bone, 1987. **8**(2): p. 95-103.
98. Cavolina, J.M., et al., *The effects of orbital spaceflight on bone histomorphometry and messenger ribonucleic acid levels for bone matrix proteins and skeletal signaling peptides in ovariectomized growing rats.* Endocrinology, 1997. **138**(4): p. 1567.
99. Westerlind, K.C., et al., *Estrogen regulates the rate of bone turnover but bone balance in ovariectomized rats is modulated by prevailing mechanical strain.* Proceedings of the National Academy of Sciences of the United States of America, 1997. **94**(8): p. 4199.
100. Cullinane, D.M. and T.A. Einhorn, *Biomechanics of bone.* Principles of bone biology, 2002. **1**: p. 17–32.
101. LeBlanc, A., et al., *Muscle volume, MRI relaxation times (T2), and body composition after spaceflight.* Journal of Applied Physiology, 2000. **89**(6): p. 2158.
102. Convertino, V.A., *Exercise and adaptation to microgravity environments.* 1996.
103. LeBlanc, A.D., et al., *Alendronate as an effective countermeasure to disuse induced bone loss.* J Musculoskelet Neuronal Interact, 2002. **2**(4): p. 335-43.
104. Mortensen, M., W. Lawson, and A. Montazem, *Osteonecrosis of the jaw associated with bisphosphonate use: presentation of seven cases and literature review.* The Laryngoscope, 2007. **117**(1): p. 30-34.
105. Silverman, S.L. and M. Maricic, *Recent developments in bisphosphonate therapy.* Semin Arthritis Rheum, 2007. **37**(1): p. 1-12.
106. Tanko, L., et al., *Oral weekly ibandronate prevents bone loss in postmenopausal women.* Journal of internal medicine, 2003. **254**(2): p. 159-167.
107. Schultheis, L., et al., *Disuse bone loss in hindquarter suspended rats: partial weightbearing, exercise and ibandronate treatment as countermeasures.* J Gravit Physiol, 2000. **7**(2): p. P13-4.
108. Ward, K., et al., *Low magnitude mechanical loading is osteogenic in children with disabling conditions.* Journal of Bone and Mineral Research, 2004. **19**(3): p. 360-369.
109. Garman, R., C. Rubin, and S. Judex, *Small oscillatory accelerations, independent of matrix deformations, increase osteoblast activity and enhance bone morphology.* PLoS ONE [Electronic Resource], 2007. **2**(7): p. 87-97.

110. Ozcivici, E., R. Garman, and S. Judex, *High-frequency oscillatory motions enhance the simulated mechanical properties of non-weight bearing trabecular bone.* Journal of biomechanics, 2007. **40**(15): p. 3404-3411.
111. Rubin, C., et al., *Prevention of Postmenopausal Bone Loss by a Low Magnitude, High Frequency Mechanical Stimuli: A Clinical Trial Assessing Compliance, Efficacy, and Safety.* Journal of Bone and Mineral Research, 2004. **19**(3): p. 343-351.
112. Christiansen, B.A. and M.J. Silva, *The effect of varying magnitudes of whole-body vibration on several skeletal sites in mice.* Annals of biomedical engineering, 2006. **34**(7): p. 1149-1156.
113. Abercromby, A.F.J., et al., *Vibration exposure and biodynamic responses during whole-body vibration training.* Medicine & Science in Sports & Exercise, 2007. **39**(10): p. 1794.
114. Worthen, L.C., et al., *Key characteristics of walking correlate with bone density in individuals with chronic stroke.* Journal of rehabilitation research and development, 2005. **42**(6): p. 761.
115. Chen, C., S. Anton, and A. Helal, *A brief survey of physical activity monitoring devices.* University of Florida Tech Report MPCL-08-09, 2008.
116. Dunbar, R.I.M., *Some aspects of research design and their implications in the observational study of behaviour.* Behaviour, 1976: p. 78-98.
117. Altmann, J., *Observational study of behavior: sampling methods.* Behaviour, 1974: p. 227-267.
118. Khan, A.M., Y.K. Lee, and T.S. Kim. *Accelerometer signal-based human activity recognition using augmented autoregressive model coefficients and artificial neural nets*. 2008: IEEE.
119. Krishnan, N.C., et al. *Real time human activity recognition using tri-axial accelerometers*. 2008.
120. Wolf, K.H., et al. *Development of a fall detector and classifier based on a triaxial accelerometer demo board*. 2007.
121. Segal-Lieberman, G., et al., *Melanin-concentrating hormone is a critical mediator of the leptin-deficient phenotype.* Proceedings of the National Academy of Sciences of the United States of America, 2003. **100**(17): p. 10085.
122. Almind, K. and C.R. Kahn, *Genetic determinants of energy expenditure and insulin resistance in diet-induced obesity in mice.* Diabetes, 2004. **53**(12): p. 3274.
123. Lamont, B.J. and D.J. Drucker, *Differential Antidiabetic Efficacy of Incretin Agonists Versus DPP-4 Inhibition in High Fat–Fed Mice.* Diabetes, 2008. **57**(1): p. 190.
124. Boyce-Rustay, J.M. and A. Holmes, *Genetic inactivation of the NMDA receptor NR2A subunit has anxiolytic-and antidepressant-like effects in mice.* Neuropsychopharmacology, 2006. **31**(11): p. 2405-2414.
125. Judex, S., et al., *Combining high-resolution micro-computed tomography with material composition to define the quality of bone tissue.* Curr Osteoporos Rep, 2003. **1**(1): p. 11-9.
126. Judex, S., et al., *Quantification of adiposity in small rodents using micro-CT.* Methods, 2009.
127. Luu, Y.K., et al., *In vivo quantification of subcutaneous and visceral adiposity by micro-computed tomography in a small animal model.* Med Eng Phys, 2009. **31**(1): p. 34-41.
128. Lublinsky, S., E. Ozcivici, and S. Judex, *An automated algorithm to detect the trabecular-cortical bone interface in micro-computed tomographic images.* Calcif Tissue Int, 2007. **81**(4): p. 285-93.
129. van Rietbergen, B., et al., *A new method to determine trabecular bone elastic properties and loading using micromechanical finite-element models.* J Biomech, 1995. **28**(1): p. 69-81.
130. Busa, B., et al., *Rapid establishment of chemical and mechanical properties during lamellar bone formation.* Calcif Tissue Int, 2005. **77**(6): p. 386-94.
131. Rho, J.Y., T.Y. Tsui, and G.M. Pharr, *Elastic properties of human cortical and trabecular lamellar bone measured by nanoindentation.* Biomaterials, 1997. **18**(20): p. 1325-30.
132. Bayraktar, H.H., et al., *Comparison of the elastic and yield properties of human femoral trabecular and cortical bone tissue.* J Biomech, 2004. **37**(1): p. 27-35.

133. Wronski, T. and E. Morey, *Skeletal abnormalities in rats induced by simulated weightlessness.* Metabolic Bone Disease and Related Research, 1982. **4**(1): p. 69-75.
134. Turner, R.T., et al. *Spaceflight results in formation of defective bone*. 1985.
135. Nordin, M. and V.H. Frankel, *Basic Biomechanics of the Skeletal System (L. Glass, ed.).* 1980: p. 15-60.
136. Ciarelli, M., et al., *Evaluation of orthogonal mechanical properties and density of human trabecular bone from the major metaphyseal regions with materials testing and computed tomography.* Journal of Orthopaedic Research, 1991. **9**(5): p. 674-682.
137. Curey, J.D., *Stress Concentration in Bone.* Q. J. Micros. Sci., 1962. **103**: p. 111-133.
138. Goodier, J.N., *Concentration of stress around spherical and cylindrical inclusions and flaws.* J. Appl. Med., 1933. **55**(39).
139. Martin, R.B., *Effects of simulated weightlessness on bone properties in rats.* Journal of biomechanics, 1990. **23**(10): p. 1021-1029.
140. Backup, P., et al., *Spaceflight results in reduced mRNA levels for tissue-specific proteins in the musculoskeletal system.* American Journal of Physiology-Endocrinology And Metabolism, 1994. **266**(4): p. E567.
141. Turner, R., G. Evans, and G. Wakley, *Spaceflight results in depressed cancellous bone formation in rat humeri.* Aviation, space, and environmental medicine, 1995. **66**(8): p. 770-774.
142. Kleber, B., et al., *Structural changes in the dental hard substances and jaw bones of animals due to short-duration weightlessness.* Zahn-, Mund-, und Kieferheilkunde mit Zentralblatt, 1989. **77**(7): p. 668.
143. Lafage-Proust, M.H., et al., *Space-related bone mineral redistribution and lack of bone mass recovery after reambulation in young rats.* American Journal of Physiology-Regulatory, Integrative and Comparative Physiology, 1998. **274**(2): p. R324.
144. Simmons, D., M. Grynpas, and G. Rosenberg, *Maturation of bone and dentin matrices in rats flown on the Soviet biosatellite Cosmos 1887.* The FASEB Journal, 1990. **4**(1): p. 29.
145. Simmons, D., et al., *Effect of spaceflight on the non-weight-bearing bones of rat skeleton.* American Journal of Physiology-Regulatory, Integrative and Comparative Physiology, 1983. **244**(3): p. R319.
146. Doty, S., et al., *Morphological studies of bone and tendon.* Journal of applied physiology (Bethesda, Md.: 1985), 1992. **73**(2 Suppl): p. 10S.
147. Vailas, A., et al., *Adaptations of young adult rat cortical bone to 14 days of spaceflight.* Journal of Applied Physiology, 1992. **73**(2): p. 4S-9S.
148. Vailas, A.C., et al., *Effects of spaceflight on rat humerus geometry, biomechanics, and biochemistry.* FASEB J, 1990. **4**(1): p. 47-54.
149. Westerlind, K.C. and R.T. Turner, *The skeletal effects of spaceflight in growing rats: Tissue specific alterations in mrna levels for TGF.* Journal of Bone and Mineral Research, 1995. **10**(6): p. 843-848.
150. Zerath, E., et al., *Effects of spaceflight on bone mineralization in the rhesus monkey.* Journal of applied physiology (Bethesda, Md.: 1985), 1996. **81**(1): p. 194.
151. Donaldson, C.L., et al., *Effect of prolonged bed rest on bone mineral* 1.* Metabolism, 1970. **19**(12): p. 1071-1084.
152. Hulley, S.B., et al., *The effect of supplemental oral phosphate on the bone mineral changes during prolonged bed rest.* Journal of Clinical Investigation, 1971. **50**(12): p. 2506.